A finite element error analysis for axisymmetric mean curvature flow*

John W. Barrett† Klaus Deckelnick‡ Robert Nürnberg†

Abstract

We consider the numerical approximation of axisymmetric mean curvature flow with the help of linear finite elements. In the case of a closed genus-1 surface, we derive optimal error bounds with respect to the L^2– and H^1–norms for a fully discrete approximation. We perform convergence experiments to confirm the theoretical results, and also present numerical simulations for some genus-0 and genus-1 surfaces, including for the Angenent torus.

Key words. mean curvature flow, axisymmetry, finite element method, error analysis, Angenent torus

AMS subject classifications. 65M60, 65M12, 65M15, 53C44, 35K55

1 Introduction

Mean curvature flow is one of the simplest prototypes for a geometric evolution equation, and it has been studied extensively in differential geometry and numerical analysis over the last few decades. For a family of closed hypersurfaces $(\mathcal{S}(t))_{t\geq 0} \subset \mathbb{R}^3$ this geometric evolution law is given by

$$\mathcal{V}_{\mathcal{S}} = k_m \qquad \text{on } \mathcal{S}(t)\,, \tag{1.1}$$

where $\mathcal{V}_{\mathcal{S}}$ denotes the normal velocity of $\mathcal{S}(t)$ in the direction of the normal $\vec{\nu}_{\mathcal{S}(t)}$, and k_m is the mean curvature of $\mathcal{S}(t)$, i.e. the sum of its principal curvatures. For an introduction to mean curvature flow and important results we refer to Mantegazza (2011).

The approximation of mean curvature flow for two-dimensional surfaces with the help of parametric finite elements goes back to the seminal work by Dziuk (1991), and other methods have since been proposed, see e.g. Barrett et al. (2008); Elliott and Fritz (2017). The first convergence proof for a parametric method has only very recently been obtained in Kovács et al. (2019) for a system that employs the position, the normal vector and the mean curvature as variables.

†Department of Mathematics, Imperial College London, London, SW7 2AZ, UK

‡Institut für Analysis und Numerik, Otto-von-Guericke-Universität Magdeburg, 39106 Magdeburg, Germany

*John passed away on 30 June 2019, when this manuscript was nearly completed. We dedicate this article to his memory.

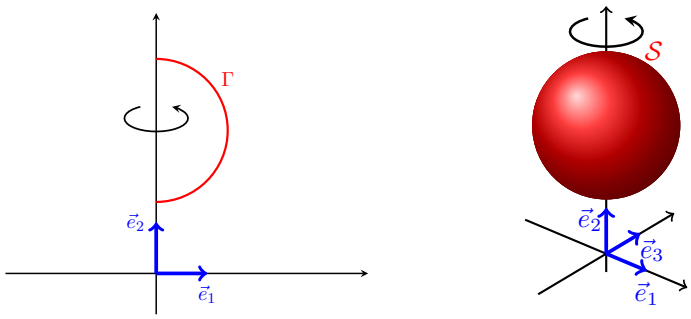

Figure 1: Sketch of Γ and $\mathcal{S}$, as well as the unit vectors $\vec{e}_1$, $\vec{e}_2$ and $\vec{e}_3$.

Optimal H^1–error bounds are proven for a spatial discretization by surface finite elements of order $k \geq 2$ and backward difference formulae for time integration. For surfaces that can be written as a graph, error bounds have previously been shown in Deckelnick and Dziuk (1995b, 2000). We refer to the review articles Deckelnick et al. (2005); Barrett et al. (2020) for further information on the numerical approximation of mean curvature flow and related geometric evolution equations, where the former article also surveys level set and phase field methods not discussed in this introduction.

In this paper we consider mean curvature flow in an axisymmetric setting. We set

$$I = \mathbb{R}/\mathbb{Z}\,, \text{ with } \partial I = \emptyset\,, \quad \text{or} \quad I = (0,1)\,, \text{ with } \partial I = \{0,1\}\,,$$

and let $\vec{x}(t) : \overline{I} \to \mathbb{R}_{\geq 0} \times \mathbb{R}$ parameterize $\Gamma(t)$, which is the generating curve of a surface $\mathcal{S}(t)$ that is axisymmetric with respect to the x_2–axis, see Figure 1. Here we allow $\Gamma(t)$ to be either a closed curve, parameterized over $\mathbb{R}/\mathbb{Z}$, which corresponds to $\mathcal{S}(t)$ being a genus-1 surface without boundary. Or $\Gamma(t)$ may be an open curve, parameterized over $[0,1]$, which corresponds to $\mathcal{S}(t)$ being a genus-0 surface, e.g. a sphere. Then the two endpoints of $\Gamma(t)$ are attached to the x_2–axis, on which they can freely move up and down. In particular, we always assume that, for all $t \in [0,T]$,

$$\vec{x}(\rho,t) \cdot \vec{e}_1 > 0 \quad \forall\ \rho \in \overline{I} \setminus \partial I\,, \tag{1.2a}$$

$$\vec{x}(\rho,t) \cdot \vec{e}_1 = 0 \quad \forall\ \rho \in \partial I\,. \tag{1.2b}$$

Let us denote by $\vec{\tau}$ and $\vec{\nu}$ a unit tangent and a unit normal to $\Gamma(t)$, respectively. It was shown in Barrett et al. (2019a) that mean curvature flow, (1.1), for an axisymmetric surface can be formulated as

$$\vec{x}_t \cdot \vec{\nu} = \varkappa - \frac{\vec{\nu} \cdot \vec{e}_1}{\vec{x} \cdot \vec{e}_1} \quad \text{in } I \times (0,T]\,, \tag{1.3a}$$

$$\vec{x}_\rho \cdot \vec{e}_2 = 0 \quad \text{on } \partial I \times (0,T]\,, \tag{1.3b}$$

where $\varkappa = \vec{\varkappa} \cdot \vec{\nu}$ and $\vec{\varkappa} = \frac{1}{|\vec{x}_\rho|} \left(\frac{\vec{x}_\rho}{|\vec{x}_\rho|} \right)_\rho$ is the curvature vector. In particular, we observe that a solution of the system

$$\vec{x}_t - \frac{1}{|\vec{x}_\rho|} \left(\frac{\vec{x}_\rho}{|\vec{x}_\rho|} \right)_\rho + \frac{\vec{\nu} \cdot \vec{e}_1}{\vec{x} \cdot \vec{e}_1}\, \vec{\nu} = \vec{0} \tag{1.4}$$

will satisfy (1.3a). Note that the leading part in the above problem is the same as in the curve shortening flow

$$\vec{x}_t - \frac{1}{|\vec{x}_\rho|} \left(\frac{\vec{x}_\rho}{|\vec{x}_\rho|} \right)_\rho = \vec{0}\,. \tag{1.5}$$

Hence it is natural to use numerical methods designed for (1.5), in order to approximate axisymmetric mean curvature flow. Optimal error bounds for a semi–discrete scheme approximating (1.5) have been obtained in Dziuk (1994), and various schemes based on (1.4) are considered in Barrett et al. (2019a), although no error analysis is given. A difficulty of the approaches using (1.5) and (1.4) lies in the fact that, in view of

$$\frac{1}{|\vec{x}_\rho|}\left(\frac{\vec{x}_\rho}{|\vec{x}_\rho|}\right)_\rho = \frac{1}{|\vec{x}_\rho|^2}\left[\vec{x}_{\rho\rho} - (\vec{x}_{\rho\rho}\cdot\vec{\tau})\,\vec{\tau}\right],$$

the resulting systems are degenerate in the tangential direction. One way to address this problem is DeTurck's trick, which essentially consists in removing this degeneracy by introducing an additional tangential motion via a suitable reparameterization. In the case of the curve shortening flow, it is natural to consider the system

$$\vec{x}_t - \frac{\vec{x}_{\rho\rho}}{|\vec{x}_\rho|^2} = \vec{0}\,, \tag{1.6}$$

for which a semi–discretization by linear finite elements was analyzed in Deckelnick and Dziuk (1995a). A whole family of schemes based on DeTurck's trick were introduced in Elliott and Fritz (2017), both for curves and surfaces. It turns out that for curves the analysis of Deckelnick and Dziuk (1995a) can be generalized to these methods.
The application of DeTurck's trick to our problem amounts to replacing (1.4) by the system

$$\vec{x}_t - \frac{\vec{x}_{\rho\rho}}{|\vec{x}_\rho|^2} + \frac{\vec{\nu}\cdot\vec{e}_1}{\vec{x}\cdot\vec{e}_1}\,\vec{\nu} = \vec{0}\,. \tag{1.7}$$

If we multiply this equation by $\vec{x}\cdot\vec{e}_1\,|\vec{x}_\rho|^2$ and note that $\vec{e}_1 = (\vec{\nu}\cdot\vec{e}_1)\,\vec{\nu} + |\vec{x}_\rho|^{-2}\,(\vec{x}_\rho\cdot\vec{e}_1)\,\vec{x}_\rho$, we are led to the following system of PDEs

$$\vec{x}\cdot\vec{e}_1\,|\vec{x}_\rho|^2\,\vec{x}_t - ((\vec{x}\cdot\vec{e}_1)\,\vec{x}_\rho)_\rho + |\vec{x}_\rho|^2\,\vec{e}_1 = \vec{0}\,, \tag{1.8}$$

on which we base the numerical scheme to be analyzed in this paper. In Section 2 we derive a weak formulation of (1.8) together with a natural fully discrete approximation using linear finite elements in space and a backward Euler scheme in time. The method is semi–implicit and hence requires the solution of a linear problem at each time step. In Section 3 we prove the main result of our paper, which are optimal error bounds both in H^1 and in L^2 in the case $I = \mathbb{R}/\mathbb{Z}$, i.e. for genus-1 surfaces. Let us remark that on using our techniques, it is straightforward to also obtain optimal L^2–error bounds for a fully discrete approximation of the curve shortening flow, something that to the best of our knowledge has not yet appeared in the literature. In Section 4 we briefly discuss an alternative formulation of axisymmetric mean curvature flow and the associated discretization. This alternative formulation has the advantage of allowing for an unconditional stability estimate for the fully discrete approximation. However, in contrast to the scheme derived in Section 2, it appears that the formulation is only well-posed in the case $I = \mathbb{R}/\mathbb{Z}$. Finally, in Section 5 we perform some numerical experiments to investigate the robustness and the accuracy of the introduced scheme, and to study some phenomena of interest in differential geometry, for example the Angenent torus.

We end this section with a few comments about notation. The L^2–inner product on I is denoted by $(\cdot,\cdot)$. We adopt the standard notation for Sobolev spaces, denoting the norm of $W^{\ell,p}(I)$ ($\ell \in \mathbb{N}_0$, $p \in [1,\infty]$) by $\|\cdot\|_{\ell,p}$ and the semi-norm by $|\cdot|_{\ell,p}$. For $p = 2$, $W^{\ell,2}(I)$ will be denoted by $H^\ell(I)$ with the associated norm and semi-norm written as, respectively, $\|\cdot\|_\ell$ and $|\cdot|_\ell$. The above

are naturally extended to vector functions, and we will write $[W^{\ell,p}(I)]^2$ for a vector function with two components. In addition, we adopt the standard notation $W^{\ell,p}(a,b;B)$ ($\ell \in \mathbb{N}$, $p \in [1,\infty]$, (a,b) an interval in $\mathbb{R}$, B a Banach space) for time dependent spaces with norm $\|\cdot\|_{W^{\ell,p}(a,b;B)}$. Once again, we write $H^\ell(a,b;B)$ if $p=2$. Furthermore, C denotes a generic positive constant independent of the mesh parameter h and the time step size Δt, see below. For later use we recall the well–known Sobolev embedding

$$|f|_{0,\infty} \leq C\,\|f\|_1 \qquad \forall\, f \in H^1(I)\,. \tag{1.9}$$

2 Weak formulation and finite element discretization

Let $\underline{V}_{\partial_0} = \{\vec\eta \in [H^1(I)]^2 : \vec\eta\cdot\vec e_1 = 0 \text{ on } \partial I\}$. A weak formulation for (1.8) is given as follows.

($\mathcal{P}$) Let $\vec x(0) \in \underline{V}_{\partial_0}$. For $t \in (0,T]$ find $\vec x(t) \in \underline{V}_{\partial_0}$ such that

$$\big((\vec x\cdot\vec e_1)\,\vec x_t, \vec\eta\,|\vec x_\rho|^2\big) + ((\vec x\cdot\vec e_1)\,\vec x_\rho, \vec\eta_\rho) + \big(\vec\eta\cdot\vec e_1, |\vec x_\rho|^2\big) = 0 \qquad \forall\,\vec\eta \in \underline{V}_{\partial_0}\,. \tag{2.1}$$

It can be shown that the weak formulation (2.1), despite the degenerate weight in the second term, weakly enforces the boundary condition (1.3b), see Barrett et al. (2019a, Appendix A) for the necessary techniques.

In order to define our finite element approximation of ($\mathcal{P}$), let $[0,1] = \bigcup_{j=1}^J I_j$, $J \geq 3$, be a decomposition of $[0,1]$ into intervals given by the nodes q_j, $I_j = [q_{j-1}, q_j]$. For simplicity we assume that the subintervals form an equipartitioning of $[0,1]$, i.e. that

$$q_j = j\,h\,, \quad \text{with} \quad h = \frac{1}{J}\,, \qquad j = 0,\ldots,J\,.$$

Clearly, if $I = \mathbb{R}/\mathbb{Z}$ we identify $0 = q_0 = q_J = 1$.

We define the finite element spaces $V^h = \{\chi \in C(\overline{I}) : \chi|_{I_j} \text{ is affine, } j=1,\ldots,J\}$, $\underline{V}^h = [V^h]^2$ and $\underline{V}^h_{\partial_0} = \underline{V}^h \cap \underline{V}_{\partial_0}$. Let $\{\chi_j\}_{j=j_0}^J$ denote the standard basis of V^h, where $j_0 = 0$ if $I = (0,1)$ and $j_0 = 1$ if $I = \mathbb{R}/\mathbb{Z}$. For later use, we let $\pi^h : C(\overline{I}) \to V^h$ be the standard interpolation operator at the nodes $\{q_j\}_{j=0}^J$. In addition, we introduce $Z^h = \{\chi \in L^\infty(I) : \chi|_{I_j} \text{ is constant, } j=1,\ldots,J\}$ and define $P^h : L^1(I) \to Z^h$ by

$$(P^h f)_{|I_j} = \frac{1}{h}\int_{I_j} f\,\mathrm{d}\rho\,, \quad j = 1,\ldots,J. \tag{2.2}$$

It is well–known that for $k \in \{0,1\}, \ell \in \{1,2\}, p \in [2,\infty]$ it holds that

$$h^{\frac{1}{p}-\frac{1}{r}}\,|\eta|_{0,r} + h\,|\eta|_{1,p} \leq C\,|\eta|_{0,p} \qquad \forall\,\eta \in V^h\,, \qquad r \in [p,\infty]\,, \tag{2.3a}$$

$$|f - \pi^h f|_{k,p} \leq C\,h^{\ell-k}\,|f|_{\ell,p} \qquad \forall\, f \in W^{\ell,p}(I)\,, \tag{2.3b}$$

$$|f - P^h f|_{0,p} \leq C\,h\,|f|_{1,p} \qquad \forall\, f \in W^{1,p}(I)\,. \tag{2.3c}$$

In order to discretize in time, let $t_m = m\,\Delta t$, $m = 0,\ldots,M$, with the uniform time step $\Delta t = \frac{T}{M} > 0$. Throughout this paper, we make use of the following short hand notations. For

a function $f \in C([0,T];B)$, with some Banach space B, we let $f^m = f(t_m)$. In addition, for a sequence of functions $(g^m)_{m\in\mathbb{N}_0}$, $g^m \in B$, we let

$$D_t g^{m+1} = \frac{g^{m+1}-g^m}{\Delta t}\,.$$

For two sequences, $(f^m)_{m\in\mathbb{N}_0}$ and $(g^m)_{m\in\mathbb{N}_0}$, we observe the discrete product rule

$$D_t(f^{m+1}\,g^{m+1}) = (D_t f^{m+1})\,g^{m+1} + f^m\,D_t g^{m+1}\,, \tag{2.4}$$

as well as the following useful summation by parts formula, for $n = 0,\ldots,M-1$:

$$\Delta t \sum_{m=0}^{n} D_t f^{m+1}\,g^m = f^{n+1}\,g^n - \Delta t \sum_{m=1}^{n} f^m\,D_t g^m, \quad \text{if } f^0 = 0\,. \tag{2.5}$$

Moreover, it is not difficult to show that for any $f \in H^1(0,T;L^2(I))$ it holds that

$$\Delta t \sum_{m=k}^{n} |D_t f^{m+1}|_0^2 \leq \int_{t_k}^{t_{n+1}} |f_t|_0^2 \,\mathrm{d}t\,, \quad 0 \leq k \leq n \leq M-1\,. \tag{2.6}$$

Our fully discrete finite element approximation of (2.1) is given as follows.

($\mathcal{P}^{h,\Delta t}$) Let $\vec{X}^0 = \pi^h \vec{x}(0) \in \underline{V}^h_{\partial_0}$. For $m = 0,\ldots,M-1$, find $\vec{X}^{m+1} \in \underline{V}^h_{\partial_0}$, such that

$$\Big((\vec{X}^m\cdot\vec{e}_1)\,D_t\vec{X}^{m+1},\vec{\eta}\,|\vec{X}^m_\rho|^2\Big) + \Big((\vec{X}^m\cdot\vec{e}_1)\,\vec{X}^{m+1}_\rho,\vec{\eta}_\rho\Big) + \Big(\vec{\eta}\cdot\vec{e}_1,|\vec{X}^m_\rho|^2\Big) = 0 \quad \forall\,\vec{\eta}\in\underline{V}^h_{\partial_0}\,. \tag{2.7}$$

Lemma. 2.1. *Let $\vec{X}^m \in \underline{V}^h_{\partial_0}$ with $\vec{X}^m\cdot\vec{e}_1 > 0$ and $|\vec{X}^m_\rho| > 0$ in I. Then there exists a unique solution $\vec{X}^{m+1} \in \underline{V}^h_{\partial_0}$ to (2.7).*

Proof. As (2.7) is a linear system, where the number of unknowns equals the number of equations, it is enough to show uniqueness. We hence consider the homogeneous system and assume that $\vec{X} \in \underline{V}^h_{\partial_0}$ is such that

$$\Big((\vec{X}^m\cdot\vec{e}_1)\,\vec{X},\vec{\eta}\,|\vec{X}^m_\rho|^2\Big) + \Delta t\,\Big((\vec{X}^m\cdot\vec{e}_1)\,\vec{X}_\rho,\vec{\eta}_\rho\Big) = 0 \quad \forall\,\vec{\eta}\in\underline{V}^h_{\partial_0}\,. \tag{2.8}$$

Choosing $\vec{\eta} = \vec{X}$ in (2.8) yields that

$$\Big(\vec{X}^m\cdot\vec{e}_1\,|\vec{X}|^2,|\vec{X}^m_\rho|^2\Big) + \Delta t\,\Big(\vec{X}^m\cdot\vec{e}_1,|\vec{X}_\rho|^2\Big) = 0\,,$$

and our assumptions on $\vec{X}^m$ imply that $\vec{X} = \vec{0}$. ∎

We are now in a position to formulate the main result of this paper, which are optimal H^1– and L^2–error bounds in the case of genus-1 surfaces.

Theorem. 2.2. *Let $\partial I = \emptyset$. Suppose that (1.8) has a solution $\vec{x}$ satisfying*

$$\vec{x} \in C([0,T];[W^{2,\infty}(I)]^2),\ \vec{x}_t \in L^2(0,T;[H^2(I)]^2),\ \vec{x}_{tt} \in L^2(0,T;[L^2(I)]^2)\,, \tag{2.9}$$

as well as

$$|\vec{x}_\rho| > 0, \quad \vec{x}\cdot\vec{e}_1 > 0 \quad \text{in } \overline{I}\times[0,T]\,. \tag{2.10}$$

Then there exist $h_0, \gamma \in \mathbb{R}_{>0}$ such that if $0 < h \leq h_0$ and $\Delta t \leq \gamma \sqrt{h}$, then $(\mathcal{P}^{h,\Delta t})$ has a unique solution $(\vec{X}^m)_{m=0,\ldots,M}$, and the following error bounds hold:

$$\max_{m=0,\ldots,M} |\vec{x}^m - \vec{X}^m|_0^2 + \Delta t \sum_{m=0}^{M-1} |\vec{x}_t^{m+1} - D_t \vec{X}^{m+1}|_0^2 \leq C \left(h^4 + (\Delta t)^2\right), \tag{2.11}$$

$$\max_{m=0,\ldots,M} |\vec{x}^m - \vec{X}^m|_1^2 \leq C \left(h^2 + (\Delta t)^2\right). \tag{2.12}$$

REMARK. 2.3. *At present we are not able to prove similar bounds for genus-0 surfaces. Note that in this case one has to deal in addition with the boundary conditions* (1.2b) *and* (1.3b)*, which state that the curve meets the x_2–axis at a right angle. An error analysis for curve shortening flow subject to normal contact to a given boundary has been carried out in Deckelnick and Elliott (1998), based on the formulation* (1.6)*. However, it is not straightforward to apply the corresponding analysis to our setting because of the presence of $\vec{x} \cdot \vec{e}_1$, which degenerates at the boundary. As we shall see in Section 5, the method nevertheless performs well in practice, also in the case of genus-0 surfaces.*

3 Error analysis

In this section, we prove the main result of this paper, Theorem 2.2. Hence we assume that $\partial I = \emptyset$, so that $I = \mathbb{R}/\mathbb{Z}$ and $\underline{V}^h_{\partial_0} = \underline{V}^h$. To begin, note that (2.9) and (2.10) imply that there exist constants $c_0, c_1, C_0 \in \mathbb{R}_{>0}$ such that the solution of (1.8) satisfies

$$\|\vec{x}(\cdot,t)\|_1 \leq C_0 \ \text{ in } [0,T], \quad c_0 \leq |\vec{x}_\rho| \leq C_0 \ \text{ in } I \times [0,T], \quad \vec{x} \cdot \vec{e}_1 \geq c_1 \ \text{ in } I \times [0,T]. \tag{3.1}$$

We claim that $\vec{X}^0, \ldots, \vec{X}^n$ solving $(\mathcal{P}^{h,\Delta t})$ exist uniquely for every $n \in \{0, \ldots, M\}$ and satisfy

$$\|\vec{X}^m\|_1 \leq 2\, C_0, \quad \frac{c_0}{2} \leq |\vec{X}^m_\rho| \leq 2\, C_0 \ \text{ in } I, \quad \vec{X}^m \cdot \vec{e}_1 \geq \frac{c_1}{2} \ \text{ in } I, \ \ m = 0, \ldots, n, \tag{3.2}$$

provided that $\Delta t \leq \gamma \sqrt{h}$ for a suitably chosen $\gamma > 0$. Clearly (3.1) and (2.3b) imply that the assertion holds for $n = 0$, provided that $0 < h \leq h_0$ and h_0 is sufficiently small. Now let us assume for an $n \in \{0, \ldots, M-1\}$ that $\vec{X}^m \in \underline{V}^h$, $0 \leq m \leq n$, solving (2.7) exist and satisfy (3.2). Lemma 2.1 implies the existence of $\vec{X}^{n+1}$, and we shall derive the corresponding bounds (3.2) with the help of an error analysis. To do so, let us decompose the error

$$\vec{x}^m - \vec{X}^m = (\vec{x}^m - \pi^h \vec{x}^m) + (\pi^h \vec{x}^m - \vec{X}^m) =: \vec{d}^m + \vec{E}^m. \tag{3.3}$$

We note that, for $k \in \{0,1\}$ and $p \in [2, \infty]$ we have from (2.3b), (2.9) and (2.6) that

$$|\vec{d}^m|_{k,p} \leq C\, h^{2-k}\, |\vec{x}^m|_{2,p} \leq C\, h^{2-k}, \ \ m = 0, \ldots, n, \tag{3.4a}$$

$$\Delta t \sum_{m=0}^{M-1} |D_t \vec{d}^{m+1}|_k^2 \leq C\, h^{4-2k} \int_0^T |\vec{x}_t|_2^2 \, \mathrm{d}t \leq C\, h^{4-2k}. \tag{3.4b}$$

In addition, we infer from Evans (1998, Theorem 4, Section 5.9.2) and (2.9) that

$$\vec{x}_t \in C([0,T]; [H^1(I)]^2),$$

and hence, on recalling (2.3b),

$$\|D_t\vec{x}^{m+1}\|_1 + \|D_t\pi^h\vec{x}^{m+1}\|_1 \leq C\,\|\vec{x}_t\|_{C([0,T];[H^1(I)]^2)} \leq C\,, \quad m=0,\ldots,M-1\,. \tag{3.5}$$

Furthermore, (3.2), (1.9), (2.3b) and (2.9) imply that

$$\|\vec{X}^m\|_{1,\infty} + \|\vec{E}^m\|_{1,\infty} \leq C\,, \quad m=0,\ldots,n\,. \tag{3.6}$$

We begin by taking the difference of (2.1) for $t=t_{m+1}$ and (2.7), in order to obtain the error relation

$$\begin{aligned}
&\Big((\vec{X}^m\cdot\vec{e}_1)\,D_t\vec{E}^{m+1},\vec{\eta}\,|\vec{X}^m_\rho|^2\Big) + \Big((\vec{X}^m\cdot\vec{e}_1)\,\vec{E}^{m+1}_\rho,\vec{\eta}_\rho\Big)\\
&\quad= \Big[\Big((\vec{X}^m\cdot\vec{e}_1)\,D_t\pi^h\vec{x}^{m+1},\vec{\eta}\,|\vec{X}^m_\rho|^2\Big) - \big((\vec{x}^{m+1}\cdot\vec{e}_1)\,\vec{x}^{m+1}_t,\vec{\eta}\,|\vec{x}^{m+1}_\rho|^2\big)\Big]\\
&\qquad+\Big[\Big(\vec{X}^m\cdot\vec{e}_1)\,(\pi^h\vec{x}^{m+1})_\rho,\vec{\eta}_\rho\Big) - \big((\vec{x}^{m+1}\cdot\vec{e}_1)\,\vec{x}^{m+1}_\rho,\vec{\eta}_\rho\big)\Big] + \Big(\vec{\eta}\cdot\vec{e}_1,\,|\vec{X}^m_\rho|^2-|\vec{x}^{m+1}_\rho|^2\Big)\\
&\quad=:\sum_{i=1}^3 T_i(\vec{\eta}) \qquad \forall\ \vec{\eta}\in\underline{V}^h\,.
\end{aligned}$$

If we set $\vec{\eta}=\Delta t\,D_t\vec{E}^{m+1}$ and sum over $m=0,\ldots,n$, we obtain

$$\begin{aligned}
&\Delta t\sum_{m=0}^n\Big(\vec{X}^m\cdot\vec{e}_1\,|D_t\vec{E}^{m+1}|^2,|\vec{X}^m_\rho|^2\Big) + \sum_{m=0}^n\Big((\vec{X}^m\cdot\vec{e}_1)\,\vec{E}^{m+1}_\rho,\vec{E}^{m+1}_\rho-\vec{E}^m_\rho\Big)\\
&\qquad=\Delta t\sum_{m=0}^n\sum_{i=1}^3 T_i(D_t\vec{E}^{m+1})\,.
\end{aligned}\tag{3.7}$$

Observing that

$$b\,(b-a)\geq\tfrac12\,(b^2-a^2)\quad\forall\ a,b\in\mathbb{R}\,, \tag{3.8}$$

and using (2.5) with $\vec{E}^0=\vec{0}$, we obtain that

$$\begin{aligned}
\sum_{m=0}^n\Big((\vec{X}^m\cdot\vec{e}_1)\,\vec{E}^{m+1}_\rho,\vec{E}^{m+1}_\rho-\vec{E}^m_\rho\Big) &\geq \tfrac12\sum_{m=0}^n\Big(\vec{X}^m\cdot\vec{e}_1,|\vec{E}^{m+1}_\rho|^2-|\vec{E}^m_\rho|^2\Big)\\
&=\tfrac12\Big(\vec{X}^n\cdot\vec{e}_1,|\vec{E}^{n+1}_\rho|^2\Big)-\tfrac12\,\Delta t\sum_{m=1}^n\Big(D_t\vec{X}^m\cdot\vec{e}_1,\,|\vec{E}^m_\rho|^2\Big)\,.
\end{aligned}$$

Combining this with (3.7) yields, on recalling (3.2), that

$$\begin{aligned}
&\frac{c_0^2\,c_1}{8}\,\Delta t\sum_{m=0}^n|D_t\vec{E}^{m+1}|_0^2+\frac{c_1}{4}\,|\vec{E}^{n+1}_\rho|_0^2\\
&\qquad\leq\tfrac12\,\Delta t\sum_{m=1}^n\Big(D_t\vec{X}^m\cdot\vec{e}_1,|\vec{E}^m_\rho|^2\Big)+\Delta t\sum_{m=0}^n\sum_{i=1}^3 T_i(D_t\vec{E}^{m+1})\,.
\end{aligned}\tag{3.9}$$

In order to treat the first term on the right hand side of (3.9) we write $D_t\vec{X}^m=D_t\pi^h\vec{x}^m-D_t\vec{E}^m$. Observing that $|\vec{E}^m_\rho|_{0,\infty}+|D_t\pi^h\vec{x}^m|_{0,\infty}\leq C$ in view of (3.6), (1.9), (3.5), we deduce that

$$\begin{aligned}
\tfrac12\,\Delta t\sum_{m=1}^n\Big(D_t\vec{X}^m\cdot\vec{e}_1,|\vec{E}^m_\rho|^2\Big)&\leq C\,\Delta t\sum_{m=1}^n\Big(|D_t\pi^h\vec{x}^m|_{0,\infty}\,|\vec{E}^m_\rho|_0^2+|\vec{E}^m_\rho|_{0,\infty}\,|D_t\vec{E}^m|_0\,|\vec{E}^m_\rho|_0\Big)\\
&\leq\varepsilon\,\Delta t\sum_{m=0}^{n-1}|D_t\vec{E}^{m+1}|_0^2+C_\varepsilon\,\Delta t\sum_{m=1}^n|\vec{E}^m_\rho|_0^2\,.
\end{aligned}\tag{3.10}$$

In the above $\varepsilon > 0$ is a parameter that will later be chosen to be sufficiently small, while C_ε is a positive constant depending on ε. Next, let us write

$$\begin{aligned} T_1(D_t\vec{E}^{m+1}) &= \Big(((\vec{X}^m - \vec{x}^{m+1})\cdot\vec{e}_1)\, D_t\pi^h\vec{x}^{m+1}, D_t\vec{E}^{m+1}\,|\vec{X}_\rho^m|^2\Big) \\ &\quad + \Big((\vec{x}^{m+1}\cdot\vec{e}_1)\,(D_t\pi^h\vec{x}^{m+1} - \vec{x}_t^{m+1}), D_t\vec{E}^{m+1}\,|\vec{X}_\rho^m|^2\Big) \\ &\quad + \Big((\vec{x}^{m+1}\cdot\vec{e}_1)\,\vec{x}_t^{m+1}, D_t\vec{E}^{m+1}\left(|\vec{X}_\rho^m|^2 - |\vec{x}_\rho^{m+1}|^2\right)\Big) =: \sum_{j=1}^{3} T_1^j\,. \end{aligned} \tag{3.11}$$

Since $|\vec{X}_\rho^m|^2 \le 4\,C_0^2$ in I, we obtain with the help of (1.9) and (3.5) that

$$\begin{aligned} \Delta t\sum_{m=0}^{n} T_1^1 &\le C\,\Delta t\sum_{m=0}^{n} |\vec{x}^{m+1} - \vec{X}^m|_0\,|D_t\pi^h\vec{x}^{m+1}|_{0,\infty}\,|D_t\vec{E}^{m+1}|_0 \\ &\le C\,\Delta t\sum_{m=0}^{n} |\vec{x}^{m+1} - \vec{X}^m|_0\,|D_t\vec{E}^{m+1}|_0 \\ &\le \varepsilon\,\Delta t\sum_{m=0}^{n} |D_t\vec{E}^{m+1}|_0^2 + C_\varepsilon\,\Delta t\sum_{m=0}^{n} |\vec{x}^{m+1} - \vec{X}^m|_0^2\,. \end{aligned} \tag{3.12}$$

For the last term in the above relation we observe that

$$\vec{x}^{m+1} - \vec{X}^m = \vec{E}^m + \vec{d}^n + \Delta t\, D_t\vec{x}^{m+1}\,, \tag{3.13}$$

so that we may infer from (3.12), together with (3.5) and (3.4a), that

$$\Delta t\sum_{m=0}^{n} T_1^1 \le \varepsilon\,\Delta t\sum_{m=0}^{n} |D_t\vec{E}^{m+1}|_0^2 + C_\varepsilon\,\Delta t\sum_{m=1}^{n} |\vec{E}^m|_0^2 + C_\varepsilon\left(h^4 + (\Delta t)^2\right). \tag{3.14}$$

Let us next consider T_1^2. Using (2.9) and again the fact that $|\vec{X}_\rho^m|^2 \le 4\,C_0^2$ in I, we may estimate

$$\begin{aligned} \Delta t\sum_{m=0}^{n} T_1^2 &\le C\,\Delta t\sum_{m=0}^{n} |D_t\pi^h\vec{x}^{m+1} - \vec{x}_t^{m+1}|_0\,|D_t\vec{E}^{m+1}|_0 \\ &\le \varepsilon\,\Delta t\sum_{m=0}^{n} |D_t\vec{E}^{m+1}|_0^2 + C_\varepsilon\,\Delta t\sum_{m=0}^{n} |D_t\pi^h\vec{x}^{m+1} - \vec{x}_t^{m+1}|_0^2\,. \end{aligned} \tag{3.15}$$

In view of (2.3b) we have

$$\begin{aligned} |D_t\pi^h\vec{x}^{m+1} - \vec{x}_t^{m+1}|_0 &= \left|\frac{1}{\Delta t}\int_{t_m}^{t_{m+1}} \pi^h\vec{x}_t - \vec{x}_t + \vec{x}_t - \vec{x}_t^{m+1}\,\mathrm{d}t\right|_0 \\ &\le \frac{1}{\Delta t}\int_{t_m}^{t_{m+1}} |\pi^h\vec{x}_t - \vec{x}_t|_0\,\mathrm{d}t + \frac{1}{\Delta t}\int_{t_m}^{t_{m+1}} |\vec{x}_t - \vec{x}_t^{m+1}|_0\,\mathrm{d}t \\ &\le C\,\frac{h^2}{\sqrt{\Delta t}}\left(\int_{t_m}^{t_{m+1}} |\vec{x}_t|_2^2\,\mathrm{d}t\right)^{\frac12} + \sqrt{\Delta t}\left(\int_{t_m}^{t_{m+1}} |\vec{x}_{tt}|_0^2\,\mathrm{d}t\right)^{\frac12}, \end{aligned} \tag{3.16}$$

which combined with (3.15) and (2.9) implies that

$$\Delta t\sum_{m=0}^{n} T_1^2 \le \varepsilon\,\Delta t\sum_{m=0}^{n} |D_t\vec{E}^{m+1}|_0^2 + C_\varepsilon\left(h^4 + (\Delta t)^2\right). \tag{3.17}$$

In order to treat T_1^3, recall (3.11), we write, on noting (3.13),

$$\begin{aligned}|\vec{x}_\rho^{m+1}|^2 - |\vec{X}_\rho^m|^2 &= 2\,(\vec{x}_\rho^{m+1} - \vec{X}_\rho^m)\cdot\vec{x}_\rho^{m+1} - |\vec{x}_\rho^{m+1} - \vec{X}_\rho^m|^2\\ &= 2\,\vec{E}_\rho^m\cdot\vec{x}_\rho^{m+1} + 2\,\vec{d}_\rho^m\cdot\vec{x}_\rho^{m+1} + 2\,\Delta t\,D_t\vec{x}_\rho^{m+1}\cdot\vec{x}_\rho^{m+1} - |\vec{E}_\rho^m + \vec{d}_\rho^m + \Delta t\,D_t\vec{x}_\rho^{m+1}|^2\\ &=: 2\,\vec{d}_\rho^m\cdot\vec{x}_\rho^{m+1} + u^m\,,\end{aligned} \tag{3.18}$$

where, in view of (2.9), (3.5), (3.4a) and (3.6),

$$\begin{aligned}|u^m|_0 &\le C\left(|\vec{E}_\rho^m|_0 + \Delta t\,|D_t\vec{x}_\rho^{m+1}|_0 + |\vec{E}_\rho^m|_{0,\infty}\,|\vec{E}_\rho^m|_0 + |\vec{d}_\rho^m|_{0,\infty}\,|\vec{d}_\rho^m|_0\right)\\ &\quad + C\,\Delta t\,|\vec{x}_\rho^{m+1} - \vec{x}_\rho^m|_{0,\infty}\,|D_t\vec{x}_\rho^{m+1}|_0\\ &\le C\left(|\vec{E}_\rho^m|_0 + h^2 + \Delta t\right).\end{aligned} \tag{3.19}$$

We obtain with the help of (3.18) and integration by parts that

$$\begin{aligned}\Delta t\sum_{m=0}^n T_1^3 &= -\Delta t\sum_{m=0}^n\left((\vec{x}^{m+1}\cdot\vec{e}_1)\,\vec{x}_t^{m+1}\cdot D_t\vec{E}^{m+1}, 2\,\vec{d}_\rho^m\cdot\vec{x}_\rho^{m+1} + u^m\right)\\ &= 2\,\Delta t\sum_{m=0}^n\left((\vec{x}^{m+1}\cdot\vec{e}_1)\,(\vec{x}_t^{m+1}\cdot D_t\vec{E}_\rho^{m+1})\,\vec{x}_\rho^{m+1}, \vec{d}^m\right)\\ &\quad + 2\,\Delta t\sum_{m=0}^n\left(\vec{v}^m, \vec{d}^m\right) - \Delta t\sum_{m=0}^n\left((\vec{x}^{m+1}\cdot\vec{e}_1)\,\vec{x}_t^{m+1}\cdot D_t\vec{E}^{m+1}, u^m\right),\end{aligned} \tag{3.20}$$

where

$$\begin{aligned}\vec{v}^m &= (\vec{x}_\rho^{m+1}\cdot\vec{e}_1)\,(\vec{x}_t^{m+1}\cdot D_t\vec{E}^{m+1})\,\vec{x}_\rho^{m+1} + (\vec{x}^{m+1}\cdot\vec{e}_1)\,(\vec{x}_{t,\rho}^{m+1}\cdot D_t\vec{E}^{m+1})\,\vec{x}_\rho^{m+1}\\ &\quad + (\vec{x}^{m+1}\cdot\vec{e}_1)\,(\vec{x}_t^{m+1}\cdot D_t\vec{E}^{m+1})\,\vec{x}_{\rho\rho}^{m+1}\,.\end{aligned}$$

Using Hölder's inequality, (1.9) and the fact that $\|\vec{x}^{m+1}\|_{2,\infty} + \|\vec{x}_t^{m+1}\|_1 \le C$, we have

$$|\vec{v}^m|_{0,1} \le C\,\|\vec{x}_t^{m+1}\|_1\,|D_t\vec{E}^{m+1}|_0 \le C\,|D_t\vec{E}^{m+1}|_0\,.$$

If we combine this bound with (3.19), and use (2.9) and (3.4a), we infer that

$$\begin{aligned}&2\,\Delta t\sum_{m=0}^n(\vec{v}^m, \vec{d}^m) - \Delta t\sum_{m=0}^n\left((\vec{x}^{m+1}\cdot\vec{e}_1)\,\vec{x}_t^{m+1}\cdot D_t\vec{E}^{m+1}, u^m\right)\\ &\quad\le C\,\Delta t\sum_{m=0}^n|\vec{v}^m|_{0,1}\,|\vec{d}^m|_{0,\infty} + C\,\Delta t\sum_{m=0}^n|D_t\vec{E}^{m+1}|_0\,|u^m|_0\\ &\quad\le C\,\Delta t\sum_{m=0}^n\left(|\vec{E}_\rho^m|_0 + h^2 + \Delta t\right)|D_t\vec{E}^{m+1}|_0\\ &\quad\le \varepsilon\,\Delta t\sum_{m=0}^n|D_t\vec{E}^{m+1}|_0^2 + C_\varepsilon\,\Delta t\sum_{m=1}^n|\vec{E}_\rho^m|_0^2 + C_\varepsilon\left(h^4 + (\Delta t)^2\right).\end{aligned} \tag{3.21}$$

It remains to consider the first term on the right hand side of (3.20). We deduce from (2.5) with $\vec{E}^0 = \vec{0}$, (2.9), (2.4), (3.4a), (3.4b), (2.6) and (3.5) that

$$\begin{aligned}
&\Delta t \sum_{m=0}^{n} \left((\vec{x}^{m+1} \cdot \vec{e}_1)\, (\vec{x}_t^{m+1} \cdot D_t \vec{E}_\rho^{m+1})\, \vec{x}_\rho^{m+1}, \vec{d}^m \right) \\
&\quad = \left((\vec{x}^{n+1} \cdot \vec{e}_1)\, (\vec{x}_t^{n+1} \cdot \vec{E}_\rho^{n+1})\, \vec{x}_\rho^{n+1}, \vec{d}^n \right) - \Delta t \sum_{m=1}^{n} \left(D_t[(\vec{x}^{m+1} \cdot \vec{e}_1)\, (\vec{x}_\rho^{m+1} \cdot \vec{d}^m)\, \vec{x}_t^{m+1}], \vec{E}_\rho^m \right) \\
&\quad \le C\, |\vec{E}_\rho^{n+1}|_0\, |\vec{d}^n|_0 + C\, \Delta t \sum_{m=1}^{n} \left(|\vec{d}^m|_{0,\infty} \left[|D_t \vec{x}_t^{m+1}|_0 + \|D_t \vec{x}^{m+1}\|_1 \right] + |D_t \vec{d}^m|_0\, |\vec{x}_t^m|_{0,\infty} \right) |\vec{E}_\rho^m|_0 \\
&\quad \le \varepsilon\, |\vec{E}_\rho^{n+1}|_0^2 + \Delta t \sum_{m=1}^{n} |\vec{E}_\rho^m|_0^2 + C_\varepsilon\, h^4 \,.
\end{aligned}$$

This implies together with (3.20) and (3.21) that

$$\Delta t \sum_{m=0}^{n} T_1^3 \le \varepsilon\, |\vec{E}_\rho^{n+1}|_0^2 + \varepsilon\, \Delta t \sum_{m=0}^{n} |D_t \vec{E}^{m+1}|_0^2 + C_\varepsilon\, \Delta t \sum_{m=1}^{n} |\vec{E}_\rho^m|_0^2 + C_\varepsilon \left(h^4 + (\Delta t)^2 \right). \tag{3.22}$$

Combining (3.11), (3.14), (3.17) and (3.22) we obtain that

$$\Delta t \sum_{m=0}^{n} T_1(D_t \vec{E}^{m+1}) \le \varepsilon \left(|\vec{E}_\rho^{n+1}|_0^2 + \Delta t \sum_{m=0}^{n} |D_t \vec{E}^{m+1}|_0^2 \right) + C_\varepsilon \left(\Delta t \sum_{m=1}^{n} \|\vec{E}^m\|_1^2 + h^4 + (\Delta t)^2 \right). \tag{3.23}$$

Let us next investigate the terms involving $T_2(D_t \vec{E}^{m+1})$ in (3.9). Since $\int_{I_j} (f - \pi^h f)_\rho\, \eta_\rho \, \mathrm{d}\rho = 0$ for all $\eta \in V^h$ and $j = 1, \ldots, J$, and on recalling the definitions of P^h and $\vec{d}^m$ from (2.2) and (3.3), we may write

$$\begin{aligned}
T_2(D_t \vec{E}^{m+1}) &= \left((\vec{X}^m \cdot \vec{e}_1)\, (\pi^h \vec{x}^{m+1})_\rho, D_t \vec{E}_\rho^{m+1} \right) - \left((\vec{x}^{m+1} \cdot \vec{e}_1)\, \vec{x}_\rho^{m+1}, D_t \vec{E}_\rho^{m+1} \right) \\
&= \left(((\vec{X}^m - \vec{x}^{m+1}) \cdot \vec{e}_1)\, \vec{x}_\rho^{m+1}, D_t \vec{E}_\rho^{m+1} \right) - \left((\vec{X}^m \cdot \vec{e}_1 - P^h[\vec{X}^m \cdot \vec{e}_1])\, \vec{d}_\rho^{m+1}, D_t \vec{E}_\rho^{m+1} \right) \\
&=: T_2^1 + T_2^2 \,.
\end{aligned} \tag{3.24}$$

Applying (2.5) with $\vec{E}^0 = \vec{0}$, we obtain that

$$\begin{aligned}
\Delta t \sum_{m=0}^{n} T_2^1 &= \left(((\vec{X}^n - \vec{x}^{n+1}) \cdot \vec{e}_1)\, \vec{x}_\rho^{n+1}, \vec{E}_\rho^{n+1} \right) - \Delta t \sum_{m=1}^{n} \left(D_t \left[((\vec{X}^m - \vec{x}^{m+1}) \cdot \vec{e}_1)\, \vec{x}_\rho^{m+1} \right], \vec{E}_\rho^m \right) \\
&=: \widetilde{T} - \Delta t \sum_{m=1}^{n} \widetilde{T}_2^1 \,.
\end{aligned} \tag{3.25}$$

Using the identity

$$\vec{x}^{n+1} - \vec{X}^n = \vec{d}^{n+1} + \vec{E}^{n+1} + \Delta t\, D_t \pi^h \vec{x}^{n+1} - \Delta t\, D_t \vec{E}^{n+1} \,,$$

and on recalling (2.9), (3.2), (1.9), (3.4a) and (3.5) we may estimate

$$\begin{aligned}
\widetilde{T} &\le C\, |\vec{x}^{n+1} - \vec{X}^n|_0\, |\vec{E}_\rho^{n+1}|_0 \\
&\le C \left(|\vec{d}^{n+1}|_0 + |\vec{E}^{n+1}|_0 + \Delta t\, |D_t \pi^h \vec{x}^{n+1}|_0 + \Delta t\, |D_t \vec{E}^{n+1}|_0 \right) |\vec{E}_\rho^{n+1}|_0 \\
&\le \varepsilon \left(|\vec{E}_\rho^{n+1}|_0^2 + \Delta t\, |D_t \vec{E}^{n+1}|_0^2 \right) + C_\varepsilon\, \Delta t\, |\vec{E}_\rho^{n+1}|_0^2 + C_\varepsilon\, |\vec{E}^{n+1}|_0^2 + C_\varepsilon \left(h^4 + (\Delta t)^2 \right).
\end{aligned}$$

Regarding the second term on the right hand side of (3.25), we obtain, on noting (2.4), (2.9), (3.13), (1.9), (3.5), (3.4a), (2.6) and (3.4b), that

$$\begin{aligned}
-\Delta t \sum_{m=1}^{n} \widetilde{T}_2^1 &\leq C\,\Delta t \sum_{m=1}^{n} \Big[|\vec{x}^{m+1} - \vec{X}^m|_{0,\infty}\, |D_t \vec{x}_\rho^{m+1}|_0 + |D_t(\vec{x}^{m+1} - \vec{X}^m)|_0 \Big]\, |\vec{E}_\rho^m|_0 \\
&\leq C\,\Delta t \sum_{m=1}^{n} \Big(\|\vec{E}^m\|_1 + |\vec{d}^m|_{0,\infty} + \Delta t\, \|D_t \vec{x}^{m+1}\|_1 \Big)\, |D_t \vec{x}_\rho^{m+1}|_0\, |\vec{E}_\rho^m|_0 \\
&\quad + C\,\Delta t \sum_{m=1}^{n} \Big(|D_t \vec{E}^m|_0 + |D_t \vec{d}^m|_0 + \Delta t\, |D_t D_t \vec{x}^{m+1}|_0 \Big)\, |\vec{E}_\rho^m|_0 \\
&\leq \varepsilon\,\Delta t \sum_{m=0}^{n-1} |D_t \vec{E}^{m+1}|_0^2 + C_\varepsilon\,\Delta t \sum_{m=1}^{n} \|\vec{E}^m\|_1^2 + C_\varepsilon \left(h^4 + (\Delta t)^2 \right),
\end{aligned}$$

where we used the fact that $\sum_{m=1}^{n} \Delta t\, |D_t D_t \vec{x}^{m+1}|_0^2 \leq C \int_0^T |\vec{x}_{tt}|_0^2 \,\mathrm{d}t \leq C$. If we insert the above estimates into (3.25) we deduce that

$$\begin{aligned}
\Delta t \sum_{m=0}^{n} T_2^1 &\leq (\varepsilon + C_\varepsilon\,\Delta t)\, |\vec{E}_\rho^{n+1}|_0^2 + \varepsilon\,\Delta t \sum_{m=0}^{n} |D_t \vec{E}^{m+1}|_0^2 + C_\varepsilon\, |\vec{E}^{n+1}|_0^2 \\
&\quad + C_\varepsilon\,\Delta t \sum_{m=1}^{n} \|\vec{E}^m\|_1^2 + C_\varepsilon \left(h^4 + (\Delta t)^2 \right). \qquad (3.26)
\end{aligned}$$

A further application of (2.5) yields together with (2.4), (2.3c) and (3.4a), on recalling (3.6), that

$$\begin{aligned}
\Delta t \sum_{m=0}^{n} T_2^2 &= -\Big((\vec{X}^n \cdot \vec{e}_1 - P^h[\vec{X}^n \cdot \vec{e}_1])\, \vec{d}_\rho^{n+1}, \vec{E}_\rho^{n+1} \Big) \\
&\quad + \Delta t \sum_{m=1}^{n} \Big(D_t \Big[(\vec{X}^m \cdot \vec{e}_1 - P^h[\vec{X}^m \cdot \vec{e}_1])\, \vec{d}_\rho^{m+1} \Big], \vec{E}_\rho^m \Big) \\
&\leq C\, h\, |(\vec{X}^n \cdot \vec{e}_1)_\rho|_{0,\infty}\, |\vec{d}_\rho^{n+1}|_0\, |\vec{E}_\rho^{n+1}|_0 + C\,\Delta t\, h \sum_{m=1}^{n} |(\vec{X}^m \cdot \vec{e}_1)_\rho|_{0,\infty}\, |D_t \vec{d}_\rho^{m+1}|_0\, |\vec{E}_\rho^m|_0 \\
&\quad + C\,\Delta t\, h \sum_{m=1}^{n} |D_t(\vec{X}^m \cdot \vec{e}_1)_\rho|_0\, |\vec{d}_\rho^m|_{0,\infty}\, |\vec{E}_\rho^m|_0 \\
&\leq C\, h^2\, |\vec{E}_\rho^{n+1}|_0 + C\,\Delta t \sum_{m=1}^{n} |\vec{E}_\rho^m|_0^2 + C\, h^2\,\Delta t \sum_{m=1}^{n} |D_t \vec{d}^{m+1}|_1^2 + C\,\Delta t\, h^2 \sum_{m=1}^{n} \|D_t \vec{X}^m\|_1\, |\vec{E}_\rho^m|_0 .
\end{aligned} \qquad (3.27)$$

We have that $\|D_t \vec{X}^m\|_1 \leq \|D_t \vec{E}^m\|_1 + \|D_t \pi^h \vec{x}^m\|_1 \leq C\,(h^{-1}\, |D_t \vec{E}^m|_0 + 1)$, on recalling (2.3a) and (3.5). Hence it follows from (3.27) and (3.4b) that

$$\begin{aligned}
\Delta t \sum_{m=0}^{n} T_2^2 &\leq C\, h^2\, |\vec{E}_\rho^{n+1}|_0 + C\,\Delta t \sum_{m=1}^{n} |\vec{E}_\rho^m|_0^2 + C\, h^4 + C\, h\,\Delta t \sum_{m=1}^{n} |D_t \vec{E}^m|_0\, |\vec{E}_\rho^m|_0 \\
&\leq \varepsilon \left(|\vec{E}_\rho^{n+1}|_0^2 + \Delta t \sum_{m=0}^{n-1} |D_t \vec{E}^{m+1}|_0^2 \right) + C_\varepsilon\,\Delta t \sum_{m=1}^{n} |\vec{E}_\rho^m|_0^2 + C_\varepsilon\, h^4 . \qquad (3.28)
\end{aligned}$$

If we combine (3.26) and (3.28) we obtain, on recalling (3.24), that

$$\Delta t \sum_{m=0}^{n} T_2(D_t\vec{E}^{m+1}) \leq (\varepsilon + C_\varepsilon\,\Delta t)\,|\vec{E}_\rho^{n+1}|_0^2 + \varepsilon\,\Delta t \sum_{m=0}^{n} |D_t\vec{E}^{m+1}|_0^2 + C_\varepsilon\,|\vec{E}^{n+1}|_0^2 + C_\varepsilon\,\Delta t \sum_{m=1}^{n} \|\vec{E}^m\|_1^2 + C_\varepsilon\left(h^4 + (\Delta t)^2\right). \tag{3.29}$$

The term $T_3(D_t\vec{E}^{m+1})$ can be treated in a similar way as T_1^3, and we obtain

$$\Delta t \sum_{m=0}^{n} T_3(D_t\vec{E}^{m+1}) \leq \varepsilon\,|\vec{E}_\rho^{n+1}|_0^2 + \varepsilon\,\Delta t \sum_{m=0}^{n} |D_t\vec{E}^{m+1}|_0^2 + C_\varepsilon\,\Delta t \sum_{m=1}^{n} |\vec{E}_\rho^{m}|_0^2 + C_\varepsilon\left(h^4 + (\Delta t)^2\right). \tag{3.30}$$

Let us insert (3.10), (3.23), (3.29) and (3.30) into (3.9). After first choosing $\varepsilon > 0$ and then $\Delta t > 0$ sufficiently small, we obtain

$$\frac{c_0^2\,c_1}{16}\,\Delta t \sum_{m=0}^{n} |D_t\vec{E}^{m+1}|_0^2 + \frac{c_1}{8}\,|\vec{E}_\rho^{n+1}|_0^2 \leq C\,|\vec{E}^{n+1}|_0^2 + C\,\Delta t \sum_{m=1}^{n} \|\vec{E}^m\|_1^2 + C\left(h^4 + (\Delta t)^2\right). \tag{3.31}$$

Finally, recalling that $\vec{E}^0 = \vec{0}$ we may write

$$|\vec{E}^{n+1}|_0^2 = \sum_{m=0}^{n} \left(|\vec{E}^{m+1}|_0^2 - |\vec{E}^m|_0^2\right) = \Delta t \sum_{m=0}^{n} \left(D_t\vec{E}^{m+1}, \vec{E}^m + \vec{E}^{m+1}\right),$$

and hence

$$2\,C\,|\vec{E}^{n+1}|_0^2 \leq \varepsilon\,\Delta t \sum_{m=0}^{n} |D_t\vec{E}^{m+1}|_0^2 + C_\varepsilon\,\Delta t \sum_{m=1}^{n} |\vec{E}^m|_0^2 + C_\varepsilon\,\Delta t\,|\vec{E}^{n+1}|_0^2.$$

Adding this bound to (3.31) and choosing first $\varepsilon > 0$ and then $\Delta t > 0$ sufficiently small, we deduce that

$$\Delta t \sum_{m=0}^{n} |D_t\vec{E}^{m+1}|_0^2 + \|\vec{E}^{n+1}\|_1^2 \leq C\,\Delta t \sum_{m=1}^{n} \|\vec{E}^m\|_1^2 + C\left(h^4 + (\Delta t)^2\right). \tag{3.32}$$

The same arguments as above show that (3.32) also holds with n replaced by k, for all $0 \leq k \leq n$. Hence the discrete Gronwall inequality implies that

$$\Delta t \sum_{m=0}^{n} |D_t\vec{E}^{m+1}|_0^2 + \|\vec{E}^{n+1}\|_1^2 \leq C\left(h^4 + (\Delta t)^2\right). \tag{3.33}$$

Let us use (3.33) in order to show that (3.2) holds for $\vec{X}^{n+1}$. Clearly, we have from (2.3a), (3.4a), (3.33) and $\Delta t \leq \gamma\sqrt{h}$ that

$$|\vec{X}_\rho^{n+1} - \vec{x}_\rho^{n+1}|_{0,\infty} \leq |\vec{E}_\rho^{n+1}|_{0,\infty} + |\vec{d}_\rho^{n+1}|_{0,\infty} \leq C\,h^{-\frac{1}{2}}\,|\vec{E}_\rho^{n+1}|_0 + C\,h \leq C\left(\Delta t\,h^{-\frac{1}{2}} + h\right) \leq C\,(\gamma + h). \tag{3.34}$$

Combining (3.34) and (3.1) yields that $\frac{c_0}{2} \leq |\vec{X}_\rho^{n+1}| \leq 2\,C_0$ provided that $0 < h \leq h_0$ and h_0, γ are small enough. The remaining bounds in (3.2) can be shown in a similar way, thus

completing the induction step, so that the discrete solution $(\vec{X}^m)_{m=0,\ldots,M}$ exists and satisfies (3.2) for $m = 0, \ldots, M$. Furthermore, the above error analysis yields that

$$\Delta t \sum_{m=0}^{M-1} |D_t \vec{E}^{m+1}|_0^2 + \max_{m=0,\ldots,M} \|\vec{E}^m\|_1^2 \leq C \left(h^4 + (\Delta t)^2\right). \tag{3.35}$$

The bounds for $\max_{m=0,\ldots,M} |\vec{x}^m - \vec{X}^m|_0^2$ and $\max_{m=0,\ldots,M} |\vec{x}^m - \vec{X}^m|_1^2$ in (2.11) and (2.12) now follow from (3.35), (3.3) and (3.4a). Finally, (3.35) together with (3.3) and (3.16) implies that

$$\Delta t \sum_{m=0}^{M-1} |\vec{x}_t^{m+1} - D_t \vec{X}^{m+1}|_0^2 \leq 2\,\Delta t \sum_{m=0}^{M-1} \left(|\vec{x}_t^{m+1} - D_t \pi^h \vec{x}^{m+1}|_0^2 + |D_t \vec{E}^{m+1}|_0^2 \right) \leq C \left(h^4 + (\Delta t)^2\right),$$

completing the proof of Theorem 2.2.

REMARK. 3.1. *Note that* (3.35) *yields a superconvergence result for the* H^1*–seminorm of the error, in that*

$$\max_{m=0,\ldots,M} |\pi^h \vec{x}^m - \vec{X}^m|_1 \leq C\, h^2,$$

provided that $\Delta t \leq C\, h^2$.

4 An alternative formulation

In this section we briefly consider an alternative formulation of axisymmetric mean curvature flow in the case $I = \mathbb{R}/\mathbb{Z}$. By way of motivation, let us briefly return to (2.1). In order to derive an apriori bound for the solution, a natural idea, that can be mimicked at the discrete level, is to choose $\vec{\eta} = \vec{x}_t$ as a test function. This yields

$$\left(\vec{x} \cdot \vec{e}_1\, |\vec{x}_t|^2, |\vec{x}_\rho|^2\right) + \left((\vec{x} \cdot \vec{e}_1)\, \vec{x}_\rho, (\vec{x}_t)_\rho\right) + \left(\vec{x}_t \cdot \vec{e}_1, |\vec{x}_\rho|^2\right) = 0\,,$$

and hence

$$\left(\vec{x} \cdot \vec{e}_1\, |\vec{x}_t|^2, |\vec{x}_\rho|^2\right) + \tfrac{1}{2} \frac{\mathrm{d}}{\mathrm{d}t} \left(\vec{x} \cdot \vec{e}_1, |\vec{x}_\rho|^2\right) = -\tfrac{1}{2} \left(\vec{x}_t \cdot \vec{e}_1, |\vec{x}_\rho|^2\right).$$

However, it does not seem possible to control the term on the right hand side, unless a lower bound of the form $\vec{x} \cdot \vec{e}_1 \geq c_1 > 0$ in $I \times [0,T]$ is available for the solution. It is therefore unlikely that we can prove an unconditional stability bound for a fully discrete approximation of (2.1).

However, the situation changes if we consider the equation that results from multiplying (1.8) by $\vec{x} \cdot \vec{e}_1$, i.e.

$$(\vec{x} \cdot \vec{e}_1)^2\, |\vec{x}_\rho|^2\, \vec{x}_t - (\vec{x} \cdot \vec{e}_1)((\vec{x} \cdot \vec{e}_1)\, \vec{x}_\rho)_\rho + (\vec{x} \cdot \vec{e}_1) |\vec{x}_\rho|^2\, \vec{e}_1 = \vec{0}\,. \tag{4.1}$$

As mentioned in the introduction, changing the tangential component of $\vec{x}_t$ just amounts to a reparametrization of $\Gamma(t) = \vec{x}(\overline{I}, t)$. It does not affect the evolution of $\Gamma(t)$. We utilize this fact by adding the tangential term

$$-(\vec{x} \cdot \vec{e}_1)\, (\vec{x}_\rho \cdot \vec{e}_1)\, \vec{x}_\rho$$

to (4.1), which allows us to write the second order term in derivative form, namely

$$(\vec{x} \cdot \vec{e}_1)^2\, |\vec{x}_\rho|^2\, \vec{x}_t - ((\vec{x} \cdot \vec{e}_1)^2\, \vec{x}_\rho)_\rho + (\vec{x} \cdot \vec{e}_1)\, |\vec{x}_\rho|^2\, \vec{e}_1 = \vec{0}\,. \tag{4.2}$$

A weak formulation for (4.2) then is given by

($\mathcal{Q}$) Let $\vec{x}(0) \in [H^1(I)]^2$. For $t \in (0,T]$ find $\vec{x}(t) \in [H^1(I)]^2$ such that

$$\left((\vec{x}\cdot\vec{e}_1)^2\,\vec{x}_t, \vec{\eta}\,|\vec{x}_\rho|^2\right) + \left((\vec{x}\cdot\vec{e}_1)^2\,\vec{x}_\rho, \vec{\eta}_\rho\right) + \left(\vec{x}\cdot\vec{e}_1, \vec{\eta}\cdot\vec{e}_1\,|\vec{x}_\rho|^2\right) = 0 \qquad \forall\ \vec{\eta} \in [H^1(I)]^2\,, \tag{4.3}$$

while our fully discrete approximation of (4.3) reads:

($\mathcal{Q}^{h,\Delta t}$) Let $\vec{X}^0 = \pi^h \vec{x}(0) \in \underline{V}^h$. For $m = 0, \dots, M-1$, find $\vec{X}^{m+1} \in \underline{V}^h$, such that

$$\left((\vec{X}^m\cdot\vec{e}_1)^2\,D_t\vec{X}^{m+1}, \vec{\eta}\,|\vec{X}^m_\rho|^2\right) + \left((\vec{X}^m\cdot\vec{e}_1)^2\,\vec{X}^{m+1}_\rho, \vec{\eta}_\rho\right) + \left(\vec{X}^{m+1}\cdot\vec{e}_1, \vec{\eta}\cdot\vec{e}_1\,|\vec{X}^{m+1}_\rho|^2\right) = 0$$
$$\forall\ \vec{\eta} \in \underline{V}^h\,. \tag{4.4}$$

We remark that while our scheme ($\mathcal{P}^{h,\Delta t}$), recall (2.7), requires the solution of two independent linear systems at each time step, for the approximation ($\mathcal{Q}^{h,\Delta t}$) one has to solve a coupled nonlinear system at each time step.
If we now choose $\vec{\eta} = \vec{x}_t$ in (4.3), we obtain that

$$\tfrac{1}{2}\frac{\mathrm{d}}{\mathrm{d}t}\left((\vec{x}\cdot\vec{e}_1)^2, |\vec{x}_\rho|^2\right) = \left((\vec{x}\cdot\vec{e}_1)^2\,\vec{x}_\rho, (\vec{x}_t)_\rho\right) + \left(\vec{x}\cdot\vec{e}_1, \vec{x}_t\cdot\vec{e}_1\,|\vec{x}_\rho|^2\right) = -\left((\vec{x}\cdot\vec{e}_1)^2\,|\vec{x}_t|^2, |\vec{x}_\rho|^2\right) \le 0\,,$$

from which we immediately obtain an apriori estimate for the solution. Mimicking the same testing procedure on the discrete level yields the following unconditional stability result.

LEMMA. 4.1. *Let $(\vec{X}^m)_{m=0,\dots,M}$ be a solution to ($\mathcal{Q}^{h,\Delta t}$). Then it holds that*

$$\tfrac{1}{2}\left((\vec{X}^{m+1}\cdot\vec{e}_1)^2, |\vec{X}^{m+1}_\rho|^2\right) + \Delta t\left((\vec{X}^m\cdot\vec{e}_1)^2\,|D_t\vec{X}^{m+1}|^2, |\vec{X}^m_\rho|^2\right) \le \tfrac{1}{2}\left((\vec{X}^m\cdot\vec{e}_1)^2, |\vec{X}^m_\rho|^2\right), \tag{4.5}$$

for $m = 0, \dots, M-1$. In particular, for $n \in \{0, \dots, M-1\}$ we have that

$$\tfrac{1}{2}\left((\vec{X}^{n+1}\cdot\vec{e}_1)^2, |\vec{X}^{n+1}_\rho|^2\right) + \Delta t\sum_{m=0}^{n}\left((\vec{X}^m\cdot\vec{e}_1)^2\,|D_t\vec{X}^{m+1}|^2, |\vec{X}^m_\rho|^2\right) \le \tfrac{1}{2}\left((\vec{X}^0\cdot\vec{e}_1)^2, |\vec{X}^0_\rho|^2\right). \tag{4.6}$$

Proof. Choosing $\vec{\eta} = \Delta t\, D_t\vec{X}^{m+1}$ in (4.4) and recalling (3.8) yields that

$$\begin{aligned}
0 &= \Delta t\left((\vec{X}^m\cdot\vec{e}_1)^2\,|D_t\vec{X}^{m+1}|^2, |\vec{X}^m_\rho|^2\right) + \left((\vec{X}^m\cdot\vec{e}_1)^2\,\vec{X}^{m+1}_\rho, (\vec{X}^{m+1}-\vec{X}^m)_\rho\right)\\
&\quad + \left(\vec{X}^{m+1}\cdot\vec{e}_1, (\vec{X}^{m+1}-\vec{X}^m)\cdot\vec{e}_1\,|\vec{X}^{m+1}_\rho|^2\right)\\
&\ge \Delta t\left((\vec{X}^m\cdot\vec{e}_1)^2\,|D_t\vec{X}^{m+1}|^2, |\vec{X}^m_\rho|^2\right) + \tfrac{1}{2}\left((\vec{X}^m\cdot\vec{e}_1)^2, |\vec{X}^{m+1}_\rho|^2 - |\vec{X}^m_\rho|^2\right)\\
&\quad + \tfrac{1}{2}\left((\vec{X}^{m+1}\cdot\vec{e}_1)^2 - (\vec{X}^m\cdot\vec{e}_1)^2, |\vec{X}^{m+1}_\rho|^2\right)\\
&= \Delta t\left((\vec{X}^m\cdot\vec{e}_1)^2\,|D_t\vec{X}^{m+1}|^2, |\vec{X}^m_\rho|^2\right) + \tfrac{1}{2}\left((\vec{X}^{m+1}\cdot\vec{e}_1)^2, |\vec{X}^{m+1}_\rho|^2\right) - \tfrac{1}{2}\left((\vec{X}^m\cdot\vec{e}_1)^2, |\vec{X}^m_\rho|^2\right).
\end{aligned}$$

This proves (4.5). Summing for $m = 0, \dots, n$ then yields the desired result (4.6). □

We conclude this section by remarking that with the help of a Brouwer fixed point theorem, see e.g. Zeidler (1986, Prop. 2.8), it is possible to prove the existence of a solution $\vec{X}^{m+1} \in \underline{V}^h$ to (4.4), provided that Δt is chosen sufficiently small. The uniqueness of this solution can also be established. Finally, using the techniques from Section 3, we can prove that the solutions of ($\mathcal{Q}^{h,\Delta t}$) satisfy error bounds similar to the ones in Theorem 2.2.

J	$\max_{m=0,\dots,M} \lvert\vec{x}^m - \vec{X}^m\rvert_0$	EOC	$\max_{m=0,\dots,M} \lvert\vec{x}^m - \vec{X}^m\rvert_1$	EOC
32	7.8742e-03	—	3.5678e-01	—
64	1.9647e-03	2.00	1.7815e-01	1.00
128	4.9092e-04	2.00	8.9045e-02	1.00
256	1.2272e-04	2.00	4.4519e-02	1.00
512	3.0678e-05	2.00	2.2259e-02	1.00

Table 1: Errors for the convergence test for (5.1) over the time interval $[0,1]$ for the scheme $(\mathcal{P}^{h,\Delta t})$ with the additional right hand side $(\pi^h \vec{f}_{\mathcal{P}}^{m+1}, \vec{\eta})$.

J	$\max_{m=0,\dots,M} \lvert\vec{x}^m - \vec{X}^m\rvert_0$	EOC	$\max_{m=0,\dots,M} \lvert\vec{x}^m - \vec{X}^m\rvert_1$	EOC
32	8.9663e-03	—	3.5842e-01	—
64	2.2421e-03	2.00	1.7836e-01	1.01
128	5.6058e-04	2.00	8.9071e-02	1.00
256	1.4015e-04	2.00	4.4522e-02	1.00
512	3.5037e-05	2.00	2.2259e-02	1.00

Table 2: Errors for the convergence test for (5.1) over the time interval $[0,1]$ for the scheme $(\mathcal{Q}^{h,\Delta t})$ with the additional right hand side $(\pi^h \vec{f}_{\mathcal{Q}}^{m+1}, \vec{\eta})$.

5 Numerical results

5.1 Genus-1 surfaces

In order to perform a convergence experiment for an evolving torus, we compute a right hand side $\vec{f}_{\mathcal{P}}$ for (1.8) so that

$$\vec{x}(\rho,t) = \begin{pmatrix} g(t) + \cos(2\,\pi\,\rho) \\ \sin(2\,\pi\,\rho) \end{pmatrix}, \quad \text{where } g(t) = 2 + \sin(\pi\,t)\,, \tag{5.1}$$

is the solution. We then compare e.g. $\vec{x}^{m+1}$ to the discrete solution $\vec{X}^{m+1}$ of (2.7), with the added right hand side $(\pi^h \vec{f}_{\mathcal{P}}^{m+1}, \vec{\eta})$. As the time step size we choose $\Delta t = h^2$, for $h = J^{-1} = 2^{-k}$, $k = 5, \dots, 9$. The results in Table 1 confirm the optimal convergence rate from Theorem 2.2. As a comparison, we provide the corresponding computation for the scheme $(\mathcal{Q}^{h,\Delta t})$ in Table 2, where the same optimal convergence rates can be observed.

Let us next consider the initial surface given by the torus

$$\mathcal{S}(0) = \left\{ \vec{z} \in \mathbb{R}^3 : (1 - |\vec{z} - (\vec{z}\cdot\vec{e}_2)\,\vec{e}_2|)^2 + (\vec{z}\cdot\vec{e}_2)^2 = r^2 \right\}, \quad \text{where } 0 < r < 1\,,$$

and denote by T_r the time at which the solution $\mathcal{S}(t)$ of (1.1) becomes singular. It is known, see Soner and Souganidis (1993, Proposition 3), that there exists a critical value $r_0 \in (0,1)$, such that for $0 < r < r_0$ the solution shrinks to a circle at time T_r, while for $r_0 < r < 1$ it closes up the hole at time T_r. Furthermore, for $r = r_0$ these effects occur at the same time.

We first demonstrate the two different behaviours by repeating the experiments in Barrett et al. (2019a, Figs. 2, 3), see also Barrett et al. (2008, Figs. 5, 6). In particular, in the first experiment

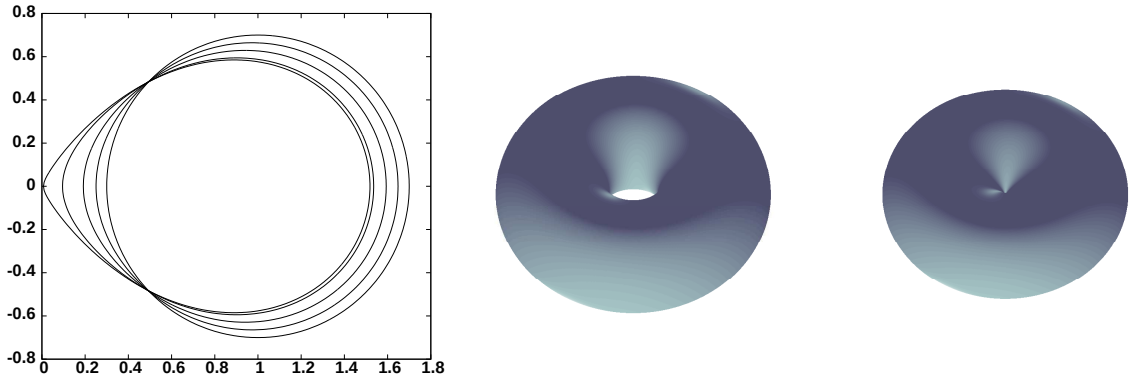

Figure 2: Evolution for a torus with $r = 0.7$. Plots are at times $t = 0, 0.025, 0.05, 0.075, 0.082$. We also visualize the axisymmetric surface $\mathcal{S}^m$ generated by Γ^m at times $t = 0$ and $t = 0.082$, where $\Gamma^m = \vec{X}^m(I)$.

we let $r = 0.7$. As expected, we obtain a surface that closes up towards a genus-0 surface, see Figure 2. As the discretization parameters we choose $J = 512$ and $\Delta t = 10^{-4}$. For the second experiment we choose a torus with $r = 0.5$ and obtain a shrinking evolution towards a circle. We show the evolution for the same discretization parameters in Figure 3. In addition, we show the evolution of the ratio

$$\mathfrak{r}^m = \frac{\max_{j=1,\dots,J} |\vec{X}^m(q_j) - \vec{X}^m(q_{j-1})|}{\min_{j=1,\dots,J} |\vec{X}^m(q_j) - \vec{X}^m(q_{j-1})|} \tag{5.2}$$

over time. We can see that compared to the corresponding ratio plots in Barrett et al. (2019a, Fig. 4), the schemes $(\mathcal{P}^{h,\Delta t})$ and $(\mathcal{Q}^{h,\Delta t})$ are performing relatively well. In particular, even close to the singularity of the flow, when the surface shrinks to a circle and then vanishes, the ratio appears to remain bounded.

To the best of our knowledge, the precise value of the critical radius r_0 is not yet known. However, we note that Ishimura (1993, Thm. 2.1), see also Ahara and Ishimura (1993), gives a rigorous proof that $r_0 \geq \frac{2}{3+\sqrt{5}} \approx 0.38$. Numerical approaches to approximate r_0 have been presented in Paolini and Verdi (1992) and Chopp (1994), with the former giving an estimate of $r_0 \approx 0.65$. In what follows, we employ our scheme $(\mathcal{P}^{h,\Delta t})$ in order to obtain an accurate approximation of r_0 by repeating the above simulations for various values of r, with the help of a bisection method. In our experiments, and with the finer discretization parameters of $J = 2048$ and $\Delta t = 10^{-5}$, we observe that r_0 appears to lie in the interval $[0.64151, 0.64152]$. We support this finding with the two simulations shown in Figure 4. We note that the stated interval for the value of r_0 is confirmed when validating it with the finer discretization parameters $J = 4096$ and $\Delta t = 5 \times 10^{-6}$.

Of particular interest in differential geometry are self-similarly shrinking solutions to the mean curvature flow, (1.1). It is clear by inspection, see also Angenent (1992), that any self-similar solution of (1.1) must be of the form

$$\mathcal{S}(t) = \left[1 - \frac{t}{\overline{T}_0}\right]^{\frac{1}{2}} \mathcal{S}(0)\,, \tag{5.3}$$

where $\overline{T}_0 > 0$ is the time at which the solution to (1.1) becomes singular. The existence of a genus-1 solution of mean curvature flow of the form (5.3) was proved by Angenent (1992).

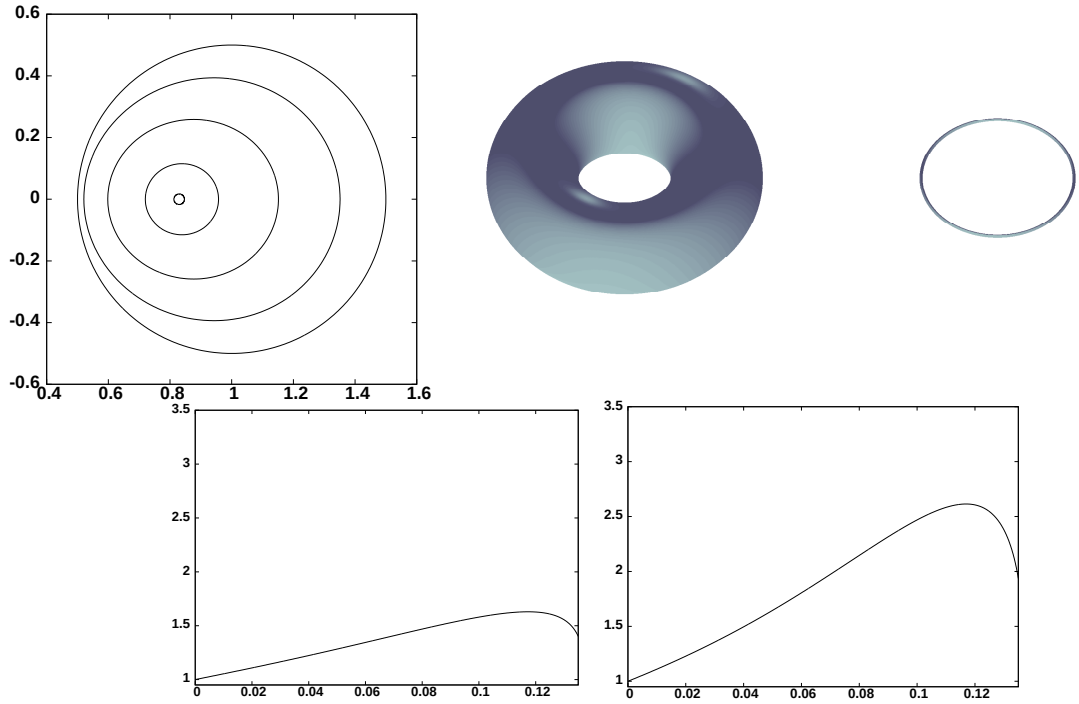

Figure 3: Evolution for a torus with $r = 0.5$. Plots are at times $t = 0, 0.05, 0.1, 0.13, 0.137$. We visualize the axisymmetric surfaces generated by Γ^m at times $t = 0$ and $t = 0.137$. Below we show plots of the ratio $\mathfrak{r}^m$ over time for the schemes ($\mathcal{P}^{h,\Delta t}$), left, and ($\mathcal{Q}^{h,\Delta t}$), right.

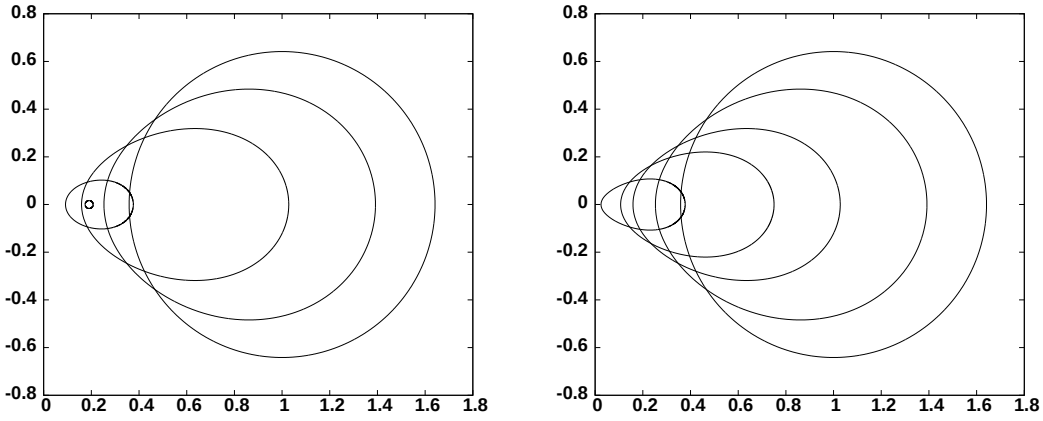

Figure 4: Evolution for a torus with $r = 0.64151$ (left) and $r = 0.64152$ (right). Plots are at times $t = 0, 0.1, 0.2, 0.25, 0.29, 0.298$ (left) and $t = 0, 0.1, 0.2, 0.25, 0.29$ (right).

The associated surface $\mathcal{S}(0)$, in the case $\overline{T}_0 = 1$, is now frequently called the Angenent torus, see e.g. Mantegazza (2011). The Angenent torus is axisymmetric, and one of its important properties is, that it is a critical point of Huisken's F-functional, see Huisken (1990), defined for a hypersurface $\mathcal{S} \subset \mathbb{R}^3$ as

$$F_{\mathcal{S}}(\mathcal{S}) = \frac{1}{4\,\pi} \int_{\mathcal{S}} e^{-\frac{1}{4}\,|\vec{\mathrm{id}}|^2}\,\mathrm{d}\mathcal{H}^2\,, \tag{5.4}$$

where $\vec{\mathrm{id}}$ denotes the identity function, and $\mathcal{H}^2$ is the two-dimensional Hausdorff measure in $\mathbb{R}^3$.

In what follows, we would like to apply the techniques introduced in this paper in order to compute approximations of the Angenent torus. To this end, we first of all note that in the axisymmetric setting, the self-similar solution (5.3) is generated by an evolving curve parameterized by $\vec{y}(t) : I \to \mathbb{R}_{\geq 0} \times \mathbb{R}$ such that

$$\vec{y}(t) = \left[1 - \frac{t}{\overline{T}_0}\right]^{\frac{1}{2}}\,\vec{y}(0)\,. \tag{5.5}$$

Clearly, (5.5) is a solution of (1.8) if and only if $\vec{y}(0)$ satisfies the elliptic equation

$$\frac{1}{2\,\overline{T}_0}\,\vec{y}\cdot\vec{e}_1\,|\vec{y}_\rho|^2\,\vec{y} + ((\vec{y}\cdot\vec{e}_1)\,\vec{y}_\rho)_\rho - |\vec{y}_\rho|^2\,\vec{e}_1 = \vec{0}\,. \tag{5.6}$$

The natural finite element approximation of (5.6), similarly to (2.7), is given by: Find $\vec{Y}^h \in \underline{V}^h$ such that

$$\mathcal{F}^h_{\overline{T}_0}(\vec{Y}^h) = \vec{0} \in \underline{V}^h\,, \tag{5.7}$$

where for $\alpha \in \mathbb{R}_{>0}$ and $\vec{\chi} \in \underline{V}^h$ we define $\mathcal{F}^h_\alpha(\vec{\chi}) \in \underline{V}^h$ via

$$\left(\mathcal{F}^h_\alpha(\vec{\chi}), \vec{\eta}\right) = \frac{1}{2\,\alpha}\left((\vec{\chi}\cdot\vec{e}_1)\,\vec{\chi}, \vec{\eta}\,|\vec{\chi}_\rho|^2\right) - \left((\vec{\chi}\cdot\vec{e}_1)\,\vec{\chi}_\rho, \vec{\eta}_\rho\right) - \left(\vec{\eta}\cdot\vec{e}_1, |\vec{\chi}_\rho|^2\right) \quad \forall\ \vec{\eta} \in \underline{V}^h\,. \tag{5.8}$$

In practice, a solution to (5.7) can be found with the help of a damped Newton iteration, provided that a suitable initial guess is used. In all our experiments for $\overline{T}_0 = 1$, the iteration converges in fewer than 10 steps when the initial value for $\vec{Y}^h$ parameterizes a circle of radius 0.6 centred around $2\,\vec{e}_1$. In Figure 5 we display some of the computed approximations to the Angenent torus for different values of J. In addition, in Figure 6 we present the evolution under mean curvature flow for the Angenent torus, by employing our scheme ($\mathcal{P}^{h,\Delta t}$) with $J = 4096$ and $\Delta t = 10^{-5}$. The presented plot nicely demonstrates the self-similar nature of the evolution, as well as the fact that the extinction time for the Angenent torus is $\overline{T}_0 = 1$.

For completeness we also compute highly accurate numerical approximations to Huisken's F-functional (5.4), as well as to the volume and the surface area of the Angenent torus, with the help of our obtained solutions $\vec{Y}^h$. To this end, let

$$\begin{aligned} F(\vec{Y}^h) &= \tfrac{1}{2}\left(\vec{Y}^h\cdot\vec{e}_1\,e^{-\frac{1}{4}\,|\vec{Y}^h|^2}, |\vec{Y}^h_\rho|\right),\\ V(\vec{Y}^h) &= \pi\left((\vec{Y}^h\,.\,\vec{e}_1)^2, [\vec{Y}^h_\rho]^\perp\,.\,\vec{e}_1\right), \quad A(\vec{Y}^h) = 2\,\pi\left(\vec{Y}^h\,.\,\vec{e}_1, |\vec{Y}^h_\rho|\right), \end{aligned}$$

where $(\cdot)^\perp$ denotes a clockwise rotation by $\frac{\pi}{2}$, and where we have used the convention that $|\vec{Y}^h_\rho|^{-1}\,(\vec{Y}^h_\rho)^\perp$ denotes the outer normal to the curve $\vec{Y}^h(I)$, see e.g. Barrett et al. (2019b) for details. In Table 3 we display these numerical approximations, together with additional characteristic properties, for different values of J. We remark that (5.4) for the Angenent torus

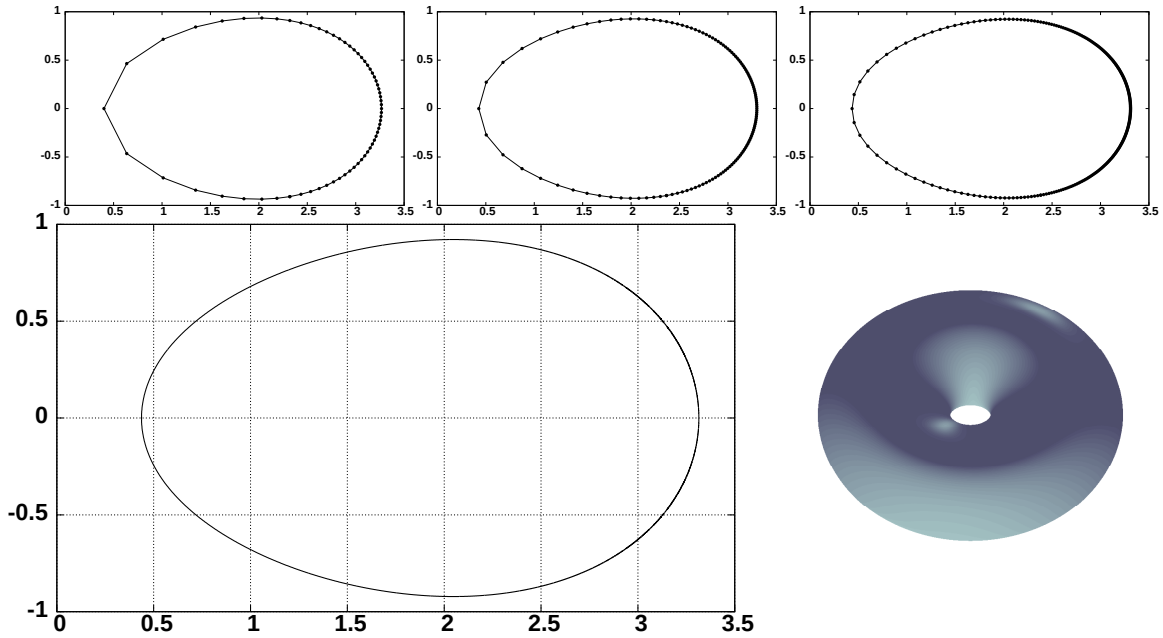

Figure 5: The solution $\vec{Y}^h$ to (5.7) for $J = 64, 128, 256$, above, and for $J = 8192$, below. We also visualize the axisymmetric surface generated by $\vec{Y}^h(I)$, for $J = 8192$.

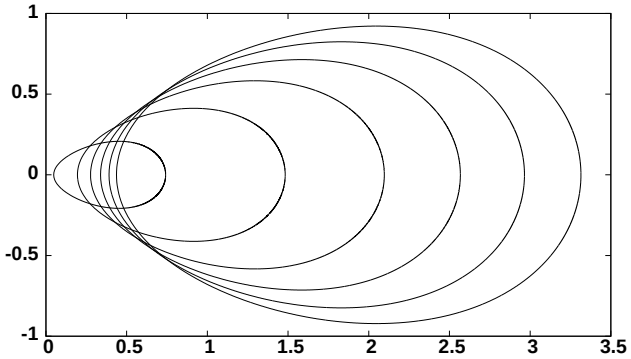

Figure 6: Evolution for the Angenent torus. Plots are at times $t = 0, 0.2, \ldots, 0.8, 0.95$.

$\log_2 J$	$F(\vec{Y}^h)$	$V(\vec{Y}^h)$	$A(\vec{Y}^h)$	$\min_I \vec{Y}^h \cdot \vec{e}_1$	$\max_I \vec{Y}^h \cdot \vec{e}_1$	$\max_I \vec{Y}^h \cdot \vec{e}_2$
16	1.8512166818	50.01714212	89.94051108	0.43712393	3.31470820	0.92171402
17	1.8512166742	50.01714302	89.94051299	0.43712396	3.31470825	0.92171401
18	1.8512166723	50.01714324	89.94051347	0.43712396	3.31470826	0.92171400
19	1.8512166718	50.01714329	89.94051359	0.43712397	3.31470827	0.92171400
20	1.8512166717	50.01714331	89.94051362	0.43712397	3.31470827	0.92171400

Table 3: Approximate values for Huisken's F-function, the enclosed volume, the surface area and the dimensions of the Angenent torus, computed with the help of the solutions $\vec{Y}^h$ to (5.7).

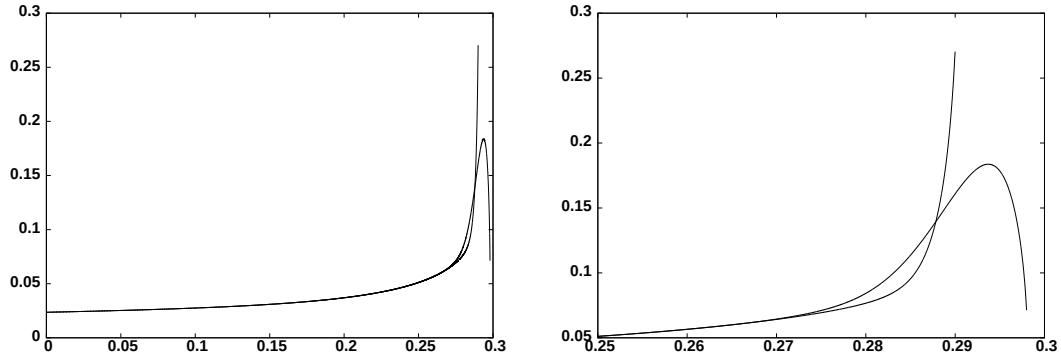

Figure 7: A plot of $G(\vec{X}^m)$ over time for the two evolutions in Figure 4. On the right a plot over the time interval $[0.25, 0.3]$.

has been approximately computed in Berchenko-Kogan (2019), with a value of 1.85122, which agrees well with our values for $F(\vec{Y}^h)$ reported in Table 3.

Finally, we are interested whether in the evolutions for the critical radius r_0 in Figure 4, the observed shapes become similar to scaled versions of the Angenent torus. To this end, we develop the following criterion for self-similarity of a given finite element approximation $\vec{Z}^h \in \underline{V}^h$. On recalling (5.8), and similarly to Chopp (1994, §3), we define the estimate for the extinction time, $\widehat{\alpha}$, and the scale-invariant goodness of a self-similarity fit, G, as

$$\widehat{\alpha}(\vec{Z}^h) = \tfrac{1}{2}\,\frac{\Big((\vec{Z}^h\cdot\vec{e}_1)^2 + (\vec{Z}^h\cdot\vec{e}_1)\,\vec{Z}^h\cdot\vec{e}_2, |\vec{Z}^h_\rho|^2\Big)}{\Big(1, |\vec{Z}^h_\rho|^2\Big)} \quad \text{and} \quad G(\vec{Z}^h) = \frac{\Big|\mathcal{F}^h_{\widehat{\alpha}(\vec{Z}^h)}(\vec{Z}^h)\Big|_0}{\widehat{\alpha}(\vec{Z}^h)}\,.$$

In Figure 7 we show the plots over time of the quantity G for the two evolutions for the critical radius in Figure 4. Throughout the evolutions, we observe that $G(\vec{X}^m) > 0.02$. Here the evolution for this quantity appears to be monotonically increasing when $r > r_0$, while for $r < r_0$ it reaches a maximum before decreasing as the torus shrinks to a circle. In comparison, the four curves in Figure 5 all satisfy $G(\vec{Y}^h) < 10^{-6}$. Hence we conjecture that the evolution for the critical radius r_0 does not approach the shape of a scaled Angenent torus at any time.

Let us finish this section with an example for mean curvature flow of a genus-1 surface that is generated from the initial data $\vec{X}^0$ parameterizing a closed spiral. As can be seen from Figure 8, the spiral slowly untangles, until the surface approaches a shrinking torus, that will once again shrink to a circle. For this experiment we use the discretization parameters $J = 1024$ and $\Delta t = 10^{-6}$, for $T = 0.029$.

5.2 Genus-0 surfaces

We recall that the error bounds in Theorem 2.2 are only shown for the case of a closed curve. Nevertheless, in this section we want to consider surfaces that are topologically equivalent to a sphere, and so $\vec{x}$ parameterizes an open curve with endpoints on the x_2–axis.

It is easy to show that a shrinking sphere with radius $[1 - 4\,t]^{\frac{1}{2}}$, which corresponds to $\overline{T}_0 = \frac{1}{4}$

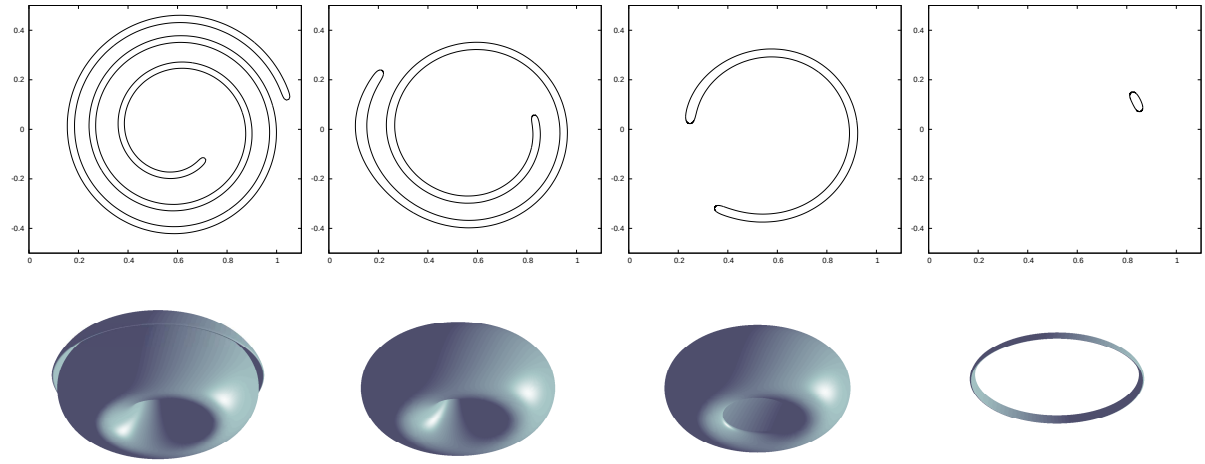

Figure 8: Evolution for a genus-1 surface generated by a spiral. Plots are at times $t = 0, 0.01, 0.02, 0.029$. Below we visualize the axisymmetric surfaces generated by the curves.

J	$\max_{m=0,\dots,M} \lvert\vec{x}^m - \vec{X}^m\rvert_0$	EOC	$\max_{m=0,\dots,M} \lvert\vec{x}^m - \vec{X}^m\rvert_1$	EOC
32	8.0301e-04	—	8.9023e-02	—
64	2.0079e-04	2.00	4.4572e-02	1.00
128	5.0199e-05	2.00	2.2285e-02	1.00
256	1.2550e-05	2.00	1.1139e-02	1.00
512	3.1375e-06	2.00	5.5674e-03	1.00

Table 4: Errors for the convergence test for (5.9) over the time interval $[0, 0.125]$ for the scheme $(\mathcal{P}^{h,\Delta t})$.

and $\mathcal{S}(0)$ being the unit sphere in (5.3), is a solution to (1.1). In fact, the parameterization

$$\vec{x}(\rho, t) = [1 - 4\,t]^{\frac{1}{2}} \begin{pmatrix} \sin(\pi\,\rho) \\ \cos(\pi\,\rho) \end{pmatrix} \tag{5.9}$$

solves (1.8). Hence we can compare e.g. $\vec{x}^{m+1}$ to the discrete solution $\vec{X}^{m+1}$ of (2.7) and perform a convergence experiment. As before, we choose $\Delta t = h^2$, for $h = J^{-1} = 2^{-k}$, $k = 5, \dots, 9$. The results in Table 4 indicate that despite the open curve case not being covered in Theorem 2.2, we still seem to observe the optimal convergence rates in practice.

We remark that the main reason we restricted our attention in Section 4 to the case of closed curves, is that it is not clear whether that alternative formulation is well-posed at the boundary. Let us give a formal justification for this observation: a smooth function satisfying (1.2b), (1.3b) will have the property that $\vec{x}_t \cdot \vec{e}_1$ is small and $\frac{\vec{x}_\rho}{|\vec{x}_\rho|}$ behaves like $\pm\vec{e}_1$ close to ∂I. Using this information in (4.2), one sees that

$$\frac{\vec{x}_{\rho\rho} \cdot \vec{x}_\rho}{|\vec{x}_\rho|^3} + \frac{1}{\vec{x} \cdot \vec{e}_1} \approx 0 \quad \text{close to } \partial I\,, \tag{5.10}$$

implying that $(\frac{1}{|\vec{x}_\rho|})_\rho$ becomes large close to ∂I. This suggests that the approach using (4.2) is not appropriate for describing the evolution of genus-0 surfaces. For the formulation (1.7), on

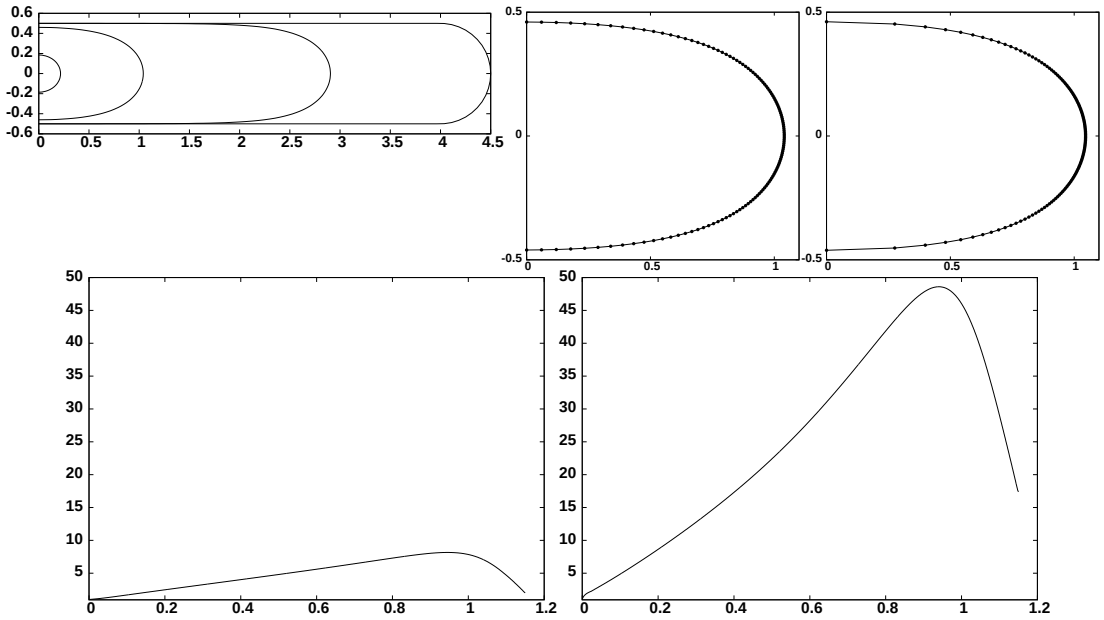

Figure 9: Evolution for a disc of dimension $9 \times 1 \times 9$. The first row shows the solution at times $t = 0, 0.5, 1, 1.15$ for the scheme $(\mathcal{P}^{h,\Delta t})$. Moreover, we present plots of the distribution of vertices on Γ^m at time $t = 1$, for the scheme $(\mathcal{P}^{h,\Delta t})$ (middle), as well as for the adapted scheme $(\mathcal{Q}^{h,\Delta t}_{\partial_0})$ (right). Below we show plots of the ratio $\mathfrak{r}^m$ over time for $(\mathcal{P}^{h,\Delta t})$, left, and for $(\mathcal{Q}^{h,\Delta t}_{\partial_0})$, right.

the other hand, we would obtain

$$\frac{\vec{x}_{\rho\rho} \cdot \vec{x}_\rho}{|\vec{x}_\rho|^3} = -\left(\frac{1}{|\vec{x}_\rho|}\right)_\rho \approx 0 \quad \text{close to } \partial I\,, \tag{5.11}$$

which is clearly satisfied by (5.9). In fact, the difference between the two formulations can be clearly seen in practice. Let $(\mathcal{Q}^{h,\Delta t}_{\partial_0})$ be the scheme $(\mathcal{Q}^{h,\Delta t})$ with $\underline{V}^h$ replaced by $\underline{V}^h_{\partial_0}$, i.e. the obvious generalisation of the scheme to the case of $I = (0, 1)$. We now compare the behaviour of this adapted scheme to $(\mathcal{P}^{h,\Delta t})$, with particular attention to the movement of the vertices near the boundary. To this end, let the initial surface be given by disc of dimension $9 \times 1 \times 9$. Under mean curvature flow, the disc shrinks to a nearly spherical shape, and then shrinks to a point, see Figure 9. For the scheme $(\mathcal{P}^{h,\Delta t})$, with discretization parameters $J = 128$ and $\Delta t = 10^{-4}$, we observe that the distribution of vertices close to the boundary remains uniform, as is to be expected from (5.11). Further away from the boundary the density of vertices increases, which leads to a moderate increase of the ratio (5.2) over time. Close to the extinction time that ratio reduces again. The scheme $(\mathcal{Q}^{h,\Delta t}_{\partial_0})$, on the other hand, exhibits a very nonuniform distribution of vertices close to the boundary, with the length of the elements increasing as the boundary is approached. Of course, this is in line with the analysis in (5.10). Overall, this leads to a far more pronounced increase in the ratio (5.2) over time, compared to the scheme $(\mathcal{P}^{h,\Delta t})$.

We end this section with an experiment for an initial dumbbell shape. For the experiment in Figure 10 we used the discretization parameters $J = 512$ and $\Delta t = 10^{-4}$. During the evolution the neck of the dumbbell is thinning, until this eventually leads to pinch-off, one of the singularities that can occur for mean curvature flow.

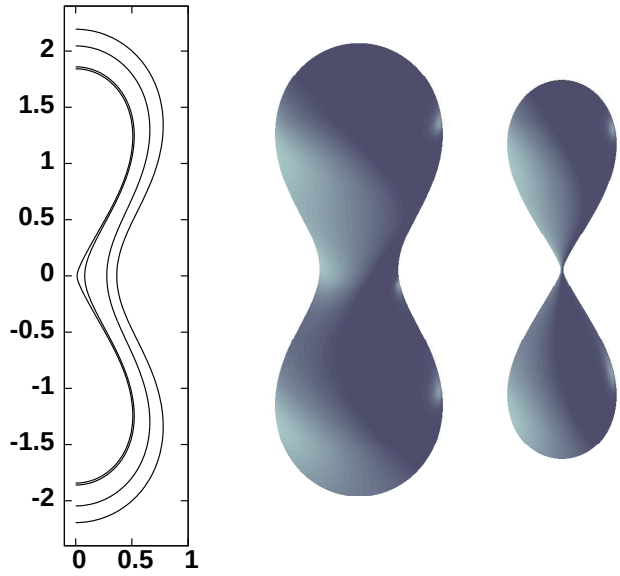

Figure 10: Evolution for a dumbbell. Solution at times $t = 0, 0.05, 0.1, 0.104$. We also visualize the axisymmetric surfaces generated by Γ^m at times $t = 0$ and $t = 0.104$.

References

K. Ahara and N. Ishimura. On the mean curvature flow of "thin" doughnuts. In *Nonlinear PDE-JAPAN Symposium 2, 1991 (Kyoto, 1991)*, volume 12 of *Lecture Notes Numer. Appl. Anal.*, pages 1–33. Kinokuniya, Tokyo, 1993.

S. B. Angenent. Shrinking doughnuts. In *Nonlinear diffusion equations and their equilibrium states, 3 (Gregynog, 1989)*, volume 7 of *Progr. Nonlinear Differential Equations Appl.*, pages 21–38. Birkhäuser Boston, Boston, MA, 1992.

J. W. Barrett, H. Garcke, and R. Nürnberg. On the parametric finite element approximation of evolving hypersurfaces in $\mathbb{R}^3$. *J. Comput. Phys.*, 227(9):4281–4307, 2008.

J. W. Barrett, H. Garcke, and R. Nürnberg. Variational discretization of axisymmetric curvature flows. *Numer. Math.*, 141(3):791–837, 2019a.

J. W. Barrett, H. Garcke, and R. Nürnberg. Finite element methods for fourth order axisymmetric geometric evolution equations. *J. Comput. Phys.*, 376:733–766, 2019b.

J. W. Barrett, H. Garcke, and R. Nürnberg. Parametric finite element approximations of curvature driven interface evolutions. In A. Bonito and R. H. Nochetto, editors, *Handb. Numer. Anal.*, volume 21, pages 275–423. Elsevier, Amsterdam, 2020.

Y. Berchenko-Kogan. The entropy of the Angenent torus is approximately 1.85122. arXiv: 1808.08163, 2019. URL `https://arxiv.org/abs/1808.08163`.

D. L. Chopp. Computation of self-similar solutions for mean curvature flow. *Experiment. Math.*, 3(1):1–15, 1994.

K. Deckelnick and G. Dziuk. On the approximation of the curve shortening flow. In C. Bandle, J. Bemelmans, M. Chipot, J. S. J. Paulin, and I. Shafrir, editors, *Calculus of Variations,*

Applications and Computations (Pont-à-Mousson, 1994), volume 326 of *Pitman Res. Notes Math. Ser.*, pages 100–108. Longman Sci. Tech., Harlow, 1995a.

K. Deckelnick and G. Dziuk. Convergence of a finite element method for non-parametric mean curvature flow. *Numer. Math.*, 72(2):197–222, 1995b.

K. Deckelnick and G. Dziuk. Error estimates for a semi-implicit fully discrete finite element scheme for the mean curvature flow of graphs. *Interfaces Free Bound.*, 2(4):341–359, 2000.

K. Deckelnick and C. M. Elliott. Finite element error bounds for a curve shrinking with prescribed normal contact to a fixed boundary. *IMA J. Numer. Anal.*, 18(4):635–654, 1998.

K. Deckelnick, G. Dziuk, and C. M. Elliott. Computation of geometric partial differential equations and mean curvature flow. *Acta Numer.*, 14:139–232, 2005.

G. Dziuk. An algorithm for evolutionary surfaces. *Numer. Math.*, 58(6):603–611, 1991.

G. Dziuk. Convergence of a semi-discrete scheme for the curve shortening flow. *Math. Models Methods Appl. Sci.*, 4(4):589–606, 1994.

C. M. Elliott and H. Fritz. On approximations of the curve shortening flow and of the mean curvature flow based on the DeTurck trick. *IMA J. Numer. Anal.*, 37(2):543–603, 2017.

L. C. Evans. *Partial differential equations*, volume 19 of *Graduate Studies in Mathematics*. American Mathematical Society, Providence, RI, 1998.

G. Huisken. Asymptotic behavior for singularities of the mean curvature flow. *J. Differential Geom.*, 31(1):285–299, 1990.

N. Ishimura. Limit shape of the cross section of shrinking doughnuts. *J. Math. Soc. Japan*, 45 (3):569–582, 1993.

B. Kovács, B. Li, and C. Lubich. A convergent evolving finite element algorithm for mean curvature flow of closed surfaces. *Numer. Math.*, 143(4):797–853, 2019.

C. Mantegazza. *Lecture notes on mean curvature flow*, volume 290 of *Progress in Mathematics*. Birkhäuser/Springer Basel AG, Basel, 2011.

M. Paolini and C. Verdi. Asymptotic and numerical analyses of the mean curvature flow with a space-dependent relaxation parameter. *Asymptotic Anal.*, 5(6):553–574, 1992.

H. M. Soner and P. E. Souganidis. Singularities and uniqueness of cylindrically symmetric surfaces moving by mean curvature. *Comm. Partial Differential Equations*, 18(5-6):859–894, 1993.

E. Zeidler. *Nonlinear Functional Analysis and its Applications. I, Fixed-Point Theorems,*. Springer-Verlag, New York, 1986.